# Application of Structure-Based Drug Design and Parallel Chemistry to Identify Selective, Brain Penetrant, In Vivo Active Phosphodiesterase 9A Inhibitors

Michelle M. Claffey,* Christopher J. Helal,* Patrick R. Verhoest, Zhijun Kang, Kristina S. Fors, Stanley Jung, Jiaying Zhong, Mark W. Bundesmann, Xinjun Hou, Shenping Lui, Robin J. Kleiman, Michelle Vanase-Frawley, Anne W. Schmidt, Frank Menniti, Christopher J. Schmidt, William E. Hoffman, Mihaly Hajos, Laura McDowell, Rebecca E. O'Connor, Mary MacDougall-Murphy, Kari R. Fonseca, Stacey L. Becker, Frederick R. Nelson, and Spiros Liras

Pfizer Worldwide Research and Development, Eastern Point Road, Groton, Connecticut 06340, United States

Ⓢ *Supporting Information*

ABSTRACT: Phosphodiesterase 9A inhibitors have shown activity in preclinical models of cognition with potential application as novel therapies for treating Alzheimer's disease. Our clinical candidate, PF-04447943 (**2**), demonstrated acceptable CNS permeability in rats with modest asymmetry between central and peripheral compartments (free brain/free plasma = 0.32; CSF/free plasma = 0.19) yet had physicochemical properties outside the range associated with traditional CNS drugs. To address the potential risk of restricted CNS penetration with **2** in human clinical trials, we sought to identify a preclinical candidate with no asymmetry in rat brain penetration and that could advance into development. Merging the medicinal chemistry strategies of structure-based design with parallel chemistry, a novel series of PDE9A inhibitors was identified that showed improved selectivity over PDE1C. Optimization afforded preclinical candidate **19** that demonstrated free brain/free plasma ≥1 in rat and reduced microsomal clearance along with the ability to increase cyclic guanosine monophosphate levels in rat CSF.
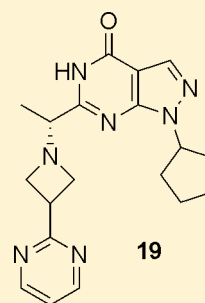
PDE9A IC$_{50}$ = 32 nM
MDR BA/AB = 1.1
C,bu/C,pu = 1
HLM Cl = 15 ml/min/kg
CNS MPO = 5.7/6

19

INTRODUCTION

Phosphodiesterases (PDEs), enzymes that catalyze the hydrolysis of the key second messenger molecules cyclic guanosine monophosphate (cGMP) and cyclic adenosine monophosphate (cAMP), have been shown to have extensive distribution in brain. On the basis of the critical nature of cyclic nucleotides in neuronal signaling, we sought to identify highly PDE subtype selective inhibitors to allow for the elucidation of the role of specific phosphodiesterates in potentially treating human neurological disease.

The identification of PDE10A, a striatal-enriched PDE that hydrolyzes both cGMP and cAMP, as a possible target for the treatment of schizophrenia, has led to a number of reports of selective and brain penetrant PDE10A inhibitors that increase cGMP levels in vivo. There exists one example of a PDE10A inhibitor that is currently in phase II clinical trials.[1]

We have more recently gained interest in other PDEs as targets, in particular PDE9A, a cGMP-specific phosphodiesterase with wide distribution throughout the brain.[2] Interestingly, the affinity of PDE9A for cGMP (K_m = ca. 170 nM) is significantly higher than that observed for other PDEs for the appropriate cyclic nucleotide. Additionally, preclinical research has shown that PDE9A inhibition can enhance cognition, thus suggesting treatment for Alzheimer's disease as well as cognitive deficits associated with schizophrenia.[3] We thus set out with the goal of identifying PDE9A inhibitors that are potent and selective to allow for a greater understanding of the biology and potential medical indications as well as to identify compounds with the appropriate alignment of potency, selectivity, permeability, clearance, and safety to consider for nomination as preclinical development candidates.

Initial efforts at identifying lead compounds utilized a combination of high-throughput screening (HTS) and corporate database searching which led to the identification of compound **1**.[4]

In addition to excellent PDE9A potency (IC$_{50}$ = 2 nM) and ligand efficiency (LE = 0.54),[5] **1** showed no efflux in a P-gp-overexpressing cell line (MDR BA/AB = 1.3), which is supportive of brain penetration, as were physicochemical properties such as molecular weight (MW = 294 AMU) and topological polar surface area (TPSA = 64 Å^2) (Figure 1).[6] A number of significant liabilities, however, also existed, such as high human liver microsomal clearance (HLM Cl) and no selectivity for PDE1C (IC$_{50}$ = 2 nM).
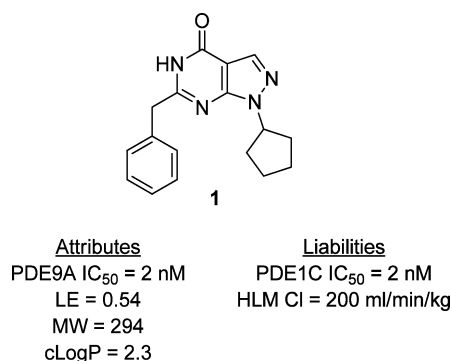
Figure 1. Structure and profile of starting PDE9A inhibitor **1**.

To efficiently address the issues with this lead, we sought to apply a number of methods simultaneously: (a) X-ray crystallographic structure-based drug design to identify critical small molecule-protein interactions, (b) parallel-enabled chemical synthesis aimed toward optimizing the key small molecule-protein interactions, and (c) prospective tracking of physicochemical properties to increase the probability of alignment of potency, selectivity, clearance, permeability, and safety.[7] We targeted HLM Cl < 20 mL/min/kg, MDR BA/AB < 2.5, and PDE9A IC_{50} < 50 nM while maintaining clogP < 3 and TPSA > 75 Å^2.[8]

Examination of the X-ray crystal structure of **1** bound to PDE9A (Figure 2) showed a number of key interactions: (a)
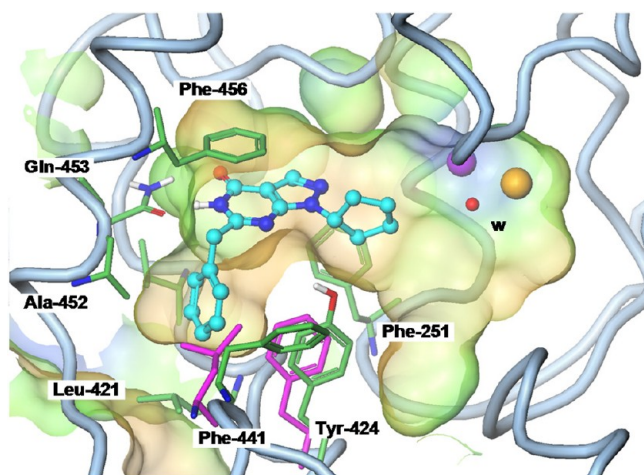

Figure 2. X-ray crystal structure of **1** bound to PDE9A (PDB 3JS1).

the pyrimidinone N—H and C=O groups of **1** formed a bidentate hydrogen bonding interaction with glutamine (Gln-453), a conserved amino acid in all PDEs that plays a critical role in cyclic nucleotide binding, (b) the bicyclic pyrazolopyrimidinone formed a π-interaction with Phe-456, (c) the benzyl substituent fit into a hydrophobic pocket comprised of Val-417, Leu-421, Phe-441, and Ala-452.

An avenue for selectivity for PDE9A over PDE1C is present in Tyr-424 (PDE9A), which is in close proximity to the inhibitor and was shown to be a Phe residue in a PDE1C homology model. Targeting this residue has successfully improved selectivity in previous work with compounds such as **2** (PF-04447943),[9] wherein the pyrrolidine nitrogen forms a hydrogen bond with a bridging water molecule to Tyr 424 while the 4-methyl group simultaneously fills the lipophilic

pocket occupied by the benzyl (Figure 3). **2** has reached phase II clinical trials.[9] Key attributes of **2** are good PDE9A potency,
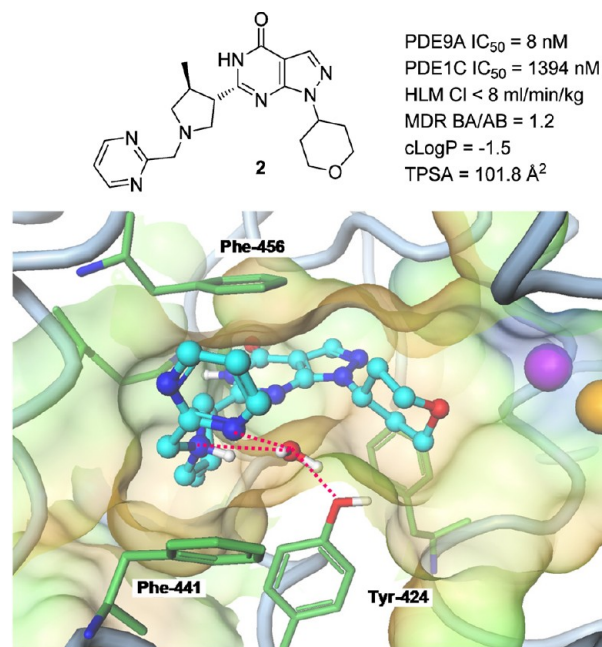

Figure 3. (top) Pyrrolidine PDE9 inhibitor PF-04447943 (**2**). (bottom) X-ray crystal structure of **2** bound to PDE9A with a water-mediated hydrogen bond to Tyr-424 via the pyrrolidine nitrogen (PDB 3JSW). Note an interaction with the N—CH$_2$ pyrimidine nitrogen in this case to the same bridging water.

high PDE selectivity, low human microsomal clearance, high in vivo oral bioavailability, and no efflux in an MDR cell line, which is predictive of acceptable CNS penetration. Measures of in vivo CNS penetration in dog reveal good central access with cerebrospinal fluid (CSF)/unbound plasma concentrations (C_{pu}) ratio = 0.9. Studies in rat demonstrated modest impairment between central and peripheral compartments with unbound brain concentration C_{bu}/C_{pu} = 0.32 and CSF/C_{pu} = 0.19. While the aggregate in vitro and in vivo CNS penetration data indicates a high probability of brain access, the physicochemical properties of **2** are outside of the traditional range for CNS drugs with a low cLogP (−1.5) and a high topological polar surface area (TPSA = 101.8 Å^2).[6b] We thus sought to identify alternative compounds that maintained many of the positive attributes of **2** but that showed no in vivo asymmetry in rat C_{bu}/C_{pu} and CSF/C_{pu} to derisk possible poor human clinical CSF drug exposure. The medicinal chemistry strategy toward this ends follows.

On the basis of molecular modeling, an alternative structure that would target both hydrogen bonding with Tyr-424 and the lipophilic pocket was devised in structure **3** (Figure 4). The basic nitrogen α to the pyrimidinone was in position to interact
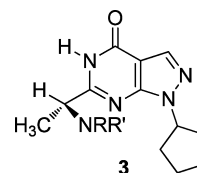

Figure 4. Design idea to address liabilities of hit **1**.

directly with the −OH of Tyr-424, and the methyl group fit into the desired lipophilic pocket. Other key design criteria that made this approach attractive were:

1. Relative to **1**, replacement of the phenyl with the methyl in **3** would reduce molecular weight and lipophilicity and could thus lead to reduced human liver microsomal clearance (HLM Cl).
2. Solubility could be improved due to low lipophilicity as well as the presence of the ionizable amine function.
3. Placement of the amine α to the electron-withdrawing pyrimidinone core would reduce the pK_a, which has shown to be advantageous in minimizing HERG ion channel affinity,[10] improving permeability, and reducing P-gp-mediated efflux.
4. Placement of the amine α to the pyrimidinone core introduces 1,3-allylic strain that would restrict the α-amino function to a major low energy conformer, thus improving the potential potency.[11]
5. A final and critical aspect was the ability to readily introduce amines at the α-position. Amines are a large and diverse monomer set which could allow for the rapid identification of optimal SAR.

Our initial goal was to prepare a chemical library of α-amine analogues **3** via S_N2 displacement of the bromide **6** (Scheme 1).
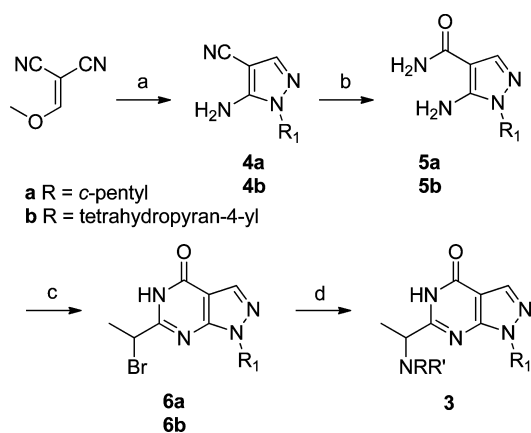
Scheme 1[a]

[a](a) R[1]-NHNH$_2$, EtOH, NaOEt, rt to reflux; (b) H$_2$O$_2$, NH$_4$OH, EtOH, rt or H$_2$SO$_4$, 0 °C to rt (60−65% over two steps); (c) (i) BrC(=O)CH(Me)Br, TEA, DMF; (ii) p-TsOH, toluene, reflux (22%); (d) HNRR′, K$_2$CO$_3$, CH$_3$CN, reflux.

This intermediate was prepared via condensation of a hydrazine with 2-(methoxymethylene)malononitrile to afford **4**. Hydrolysis of the nitrile to the primary amide under acidic conditions gave **5**. The formation of **6** was achieved via a one-pot acylation/condensation of 2-bromopropanoyl bromide with **5**. Selection of amine monomers started with the available compounds from Pfizer's in-house monomer store. A virtual library was generated with 3700 secondary amines available internally. The product library was filtered to 1658 molecules by MW < 480 and TPSA < 120 Å^2 to generate a subset with a higher probability of brain permeability. The 3-D conformation of the library was generated by Corina,[12] and multiple stereoisomers were generated for unspecified stereocenters in the amine monomers. The resulting 3-D conformers were docked into the binding site of PDE9A with the pyrimidinone core partially constrained to the crystal structure of **1** using an

in-house AGDOCK program.[13] All docked poses were rank-ordered by an in-house scoring function[14] and were followed by visual inspection. A final set of 300 compounds was selected for synthesis.

Some key SAR points from successfully synthesized library compounds are shown (Table 1). In the case of minimally

Table 1. SAR of Initial α-Amine Library

Compound	-NRR	PDE9A IC$_{50}$ (nM)	% Inhibition @ 1 uM
3a		> 1000	5
3b		> 1000	44
3c		593	-
3d		>1000	0
3e		>1000	28%
3f		230	-
3g		148	-
3h		14	-

substituted cyclic amines, piperidine (**3a**) had little activity, 3-fluoropyrrolidine (**3b**) had PDE9A IC$_{50}$ approaching 1000 nM, and azetidine (**3c**) was most active with PDE9A IC$_{50}$ = 593 nM. The potency trend of azetidine > pyrrolidine > piperidine was replicated in the case of aryl substituted variants. For example, piperidines with an aryl group fused (**3d**) or directly attached (**3e**) showed little activity. Pyrrolidines with an aryl group attached directly (**3f**) or via an oxygen linker (**3g**) were significantly more active with PDE9A IC$_{50}$ values of 230 and 148 nM, respectively. The azetidine with an oxygen linker (**3h**) gained an order of magnitude in potency relative to the pyrrolidines (PDE9A IC$_{50}$ = 14 nM).

To verify the result with **3h**, this compound was resynthesized, isolated as a solid, and was characterized (Figure 5). The retest data with **3h** (racemic) afforded a slight reduction in potency compared to the original library sample
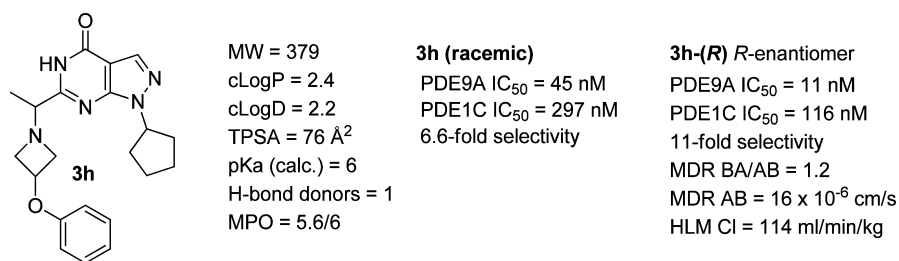
MW = 379
cLogP = 2.4
cLogD = 2.2
TPSA = 76 Å^2
pKa (calc.) = 6
H-bond donors = 1
MPO = 5.6/6

3h (racemic)
PDE9A IC$_{50}$ = 45 nM
PDE1C IC$_{50}$ = 297 nM
6.6-fold selectivity

3h-(R) *R*-enantiomer
PDE9A IC$_{50}$ = 11 nM
PDE1C IC$_{50}$ = 116 nM
11-fold selectivity
MDR BA/AB = 1.2
MDR AB = 16 x 10^{-6} cm/s
HLM Cl = 114 ml/min/kg

Figure 5. Calculated and in vitro data for resynthesized library hit **3h** and the single enantiomer **3h**-(*R*).

(PDE9A IC$_{50}$ = 45 nM). Encouragingly, improved PDE1C selectivity (6.6-fold) was observed as compared to the **1** (no selectivity).

Separation of the racemic mixture and testing of the enantiomers showed PDE9A inhibition resided with one compound (enantiomer PDE9A IC$_{50}$ = 11 and 986 nM, respectively). The X-ray crystal structure of the more active enantiomer bound to PDE9A indicated that the (*R*)-stereochemistry was present (Figure 6). A number of interesting
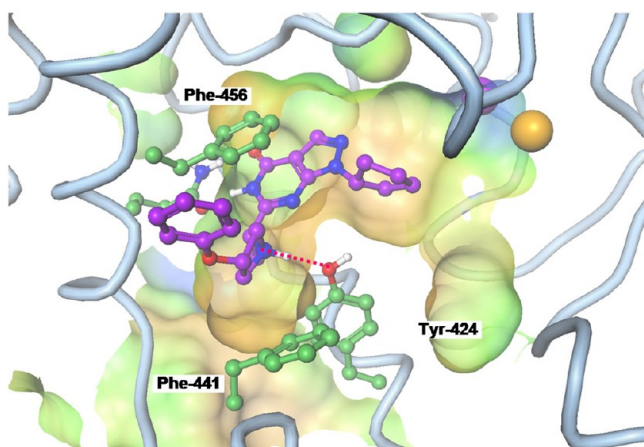

Figure 6. X-ray structure of **3h**-(*R*) bound to PDE9A (PDB 4G2J).

features were observed in that: (1) The α-methyl amine function resided in the conformation to minimize 1,3-allylic strain. (2) The α-methyl group of **3h**-(*R*) fit into the lipophilic pocket occupied by the benzyl in **1**. (3) The azetidine nitrogen formed a direct hydrogen bond with the −OH of Tyr-424 and explained the increased selectivity over PDE1C; this is in contrast to the water-bridged hydrogen bond displayed by **2**. (4) The OPh group was aligned to make an edge−face π-interaction with Phe-456.

This single enantiomer **3h**-(*R*) displayed improved potency as compared to the racemic compound **3h** (PDE9A IC$_{50}$ = 11 and 45 nM, respectively). In addition to improved potency, selectivity over PDE1C improved (11-fold), no efflux was noted in an MDR cell line,[15] and HLM Cl was high. Application of a recently developed multiparametric optimization (MPO) physicochemical analysis for neuroscience drugs suggested that the compound had excellent alignment of physical properties with an MPO score = 5.6 out of 6.[16]

To improve HLM Cl, SAR from **2** was applied wherein the cyclopentyl group in **3h**-(*R*) was changed to a 4-tetrahydropyran, which decreased cLogP and increased topological polar surface area (**7**, Figure 7). Potency against PDE9A was maintained (IC$_{50}$ = 22 nM), PDE1C selectivity was improved (>50-fold), HLM Cl decreased significantly, and excellent

MW = 395
cLogP = 0.6
cLogD = 0.89
TPSA = 85
H-bond donors = 1
pKa (calc.) = 5.8
MPO = 5.6/6

PDE9 IC$_{50}$ = 22 nM
PDE1C IC$_{50}$ >1,000 nM
HLM Cl,int = 24 ml/min/kg
MDR BA/AB = 1
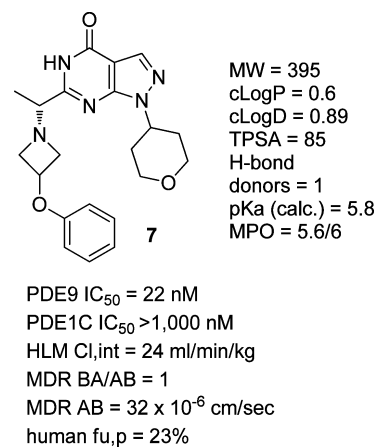MDR AB = 32 x 10^{-6} cm/sec
human fu,p = 23%

Figure 7. Merging SAR of **3h**-(*R*) and **2** yielded **7**.

permeability with no sign of P-gp-efflux was seen. Additionally, with a CNS MPO of 5.6/6, the physicochemical properties remained in excellent space. In vivo mouse brain penetration studies showed **7** to be highly brain permeable with C_{bu}/C_{pu} ratio equal to 0.6 with only moderate plasma protein binding (human fu$_p$ = 23%).[17]

In vivo, **7** was evaluated for its ability to increase rat CSF cGMP levels (Figure 8). Cyclic nucleotide levels increased with increasing dose levels, demonstrating biochemical efficacy.
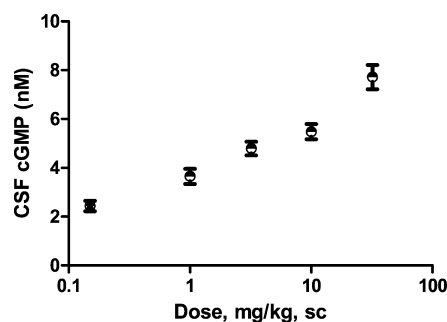

Figure 8. In vivo increases in cGMP in rat CSF with increasing doses of **7**.

On the basis of favorable potency, PDE1C selectivity, and ADME properties, **7** was evaluated in a selectivity panel against a broad range of enzymes, ion channels, transporters, etc. Besides PDE1 activity, <30% inhibition against PDE2−8, -10, and -11 was observed at a concentration of 1 μM. Significant potency against the human dopamine transporter (DAT K_i = 293 nM) was observed. However, in vivo studies in rodents showed none of the hyperactivity generally associated with

dopamine transporter blockade, suggesting that **7** may be functionally inactive.

Nonetheless, on the basis of the potential liabilities associated with DAT inhibition, we sought to design away from DAT activity in our series. Our hypothesis was that the 3-phenoxyazetidine overlapped with an established pharmacophore for DAT inhibition, 4-phenylpiperidine.[18] Pharmacophore disruption was pursued by taking advantage of the highly synthetically enabled nature of 3-phenoxyazetidines.

To vary the azetidine 3-substituent effectively, **6b** could be directly aminated with a 3-aryloxy-azetidine (Scheme 1). Alternatively, **6b** could be reacted with 3-hydroxy azetidine to afford **8**, followed by activation of the hydroxyl with methanesulfonyl chloride (**9**) and displacement of the methanesulfonate with phenols to afford compounds of general formula **10** (Scheme 2). Alternatively, the hydroxyl group of **8** could be directly functionalized under standard ether forming conditions.
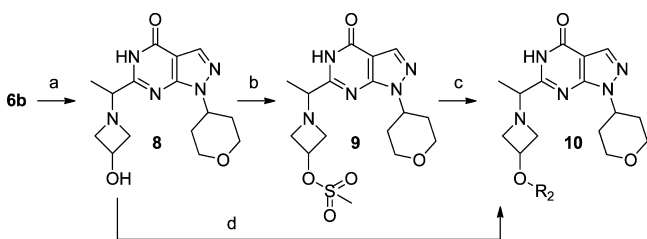
Scheme 2[a]

[a](a) amine, TEA, acetonitrile, 85−90 °C (54−70%); (b) MsCl, TEA, CH₂Cl₂ (67%); (c) R²-OH, K₂CO₃, acetonitrile, reflux, (33−85%); (d) R²-Cl or R²-Br, KOt-Bu, 70 °C (40−70%).

To make analogues in an enantiospecific manner, a variation of the existing synthetic route was devised wherein the use of commercially available (S)-1-chloro-1-oxopropan-2-yl acetate (ca. 90% ee) afforded key α-hydroxy intermediate **11** in 88% ee (Scheme 3). Activation of the hydroxyl with methanesulfonyl
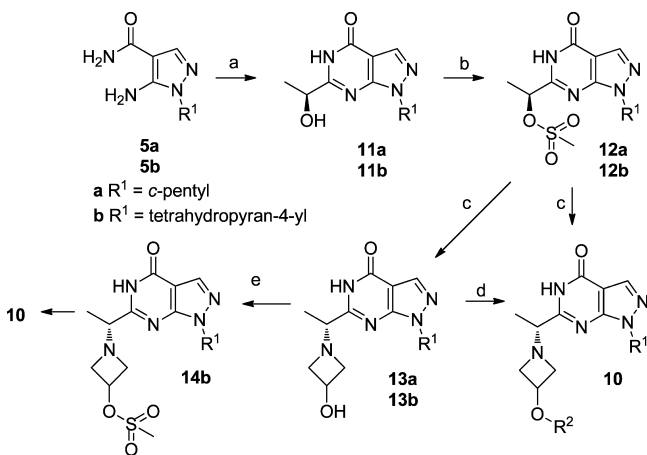
Scheme 3[a]

[a](a) (S)-1-Chloro-1-oxopropan-2-yl acetate, dioxane, reflux; H₂O, K₂CO₃, 45 °C (84−90%); (b) MsCl, triethylamine or N-methylmorpholine, 0 °C to rt (41−74%); (c) amine, TEA, acetonitrile, 85−90 °C (54−70%); (d) R²-Cl or R²-Br, KOt-Bu, 70 °C (40−70%); (e) MsCl, TEA, CH₂Cl₂ (67%); (f) R²-OH, K₂CO₃, acetonitrile, reflux, (33−85%).

chloride afforded **12**, which was subsequently treated with a free-based amine in the absence of nucleophilic counterions (e.g., chloride) to allow for highly stereoselective SN2 displacement, thus affording final compounds **10** or key intermediates such as **13**. If an amine hydrochloride salt was utilized in the displacement, significant racemization was observed due to competing SN2 attack with chloride, generating the (R)-α-chloro intermediate that could subsequently be displaced with the amine to afford the undesired (S)-amino enantiomer (see Supporting Information). As in the racemic synthesis (Scheme 2), the hydroxyl group in **13** could be directly functionalized to afford final analogues **10**. In the case of **14b**, displacement of the mesylate resulted in epimerization under the conditions used (Table 2).
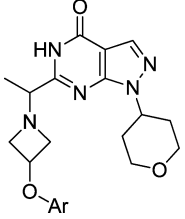
A series of analogues was prepared wherein the OR² group was varied using substituted phenols (Table 2). Halogenation of the aryl group (**10a−c**) led to no improvement in potency and increases in HLM Cl, most likely being driven by increased lipophilicity. Additionally, assessment of DAT activity showed little change (e.g., **10a** DAT K_i = 1.2 μM). The incorporation of polar functionality such as p-CN (**10d**) reduced DAT affinity significantly (K_i > 10 μM) as well as HLM Cl, but signs of increased efflux were observed in the MDR assay. To balance the increased polarity of the CN group that led to significant reduction in cLogP and potentially led to efflux, halogens were added (**10e−g**), bringing lipophilicity in line with previous compounds that did not have MDR efflux. Unfortunately, reductions in MDR efflux were not observed.
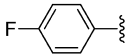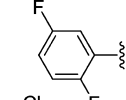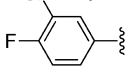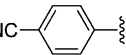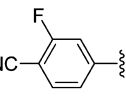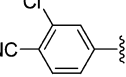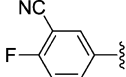
The exploration of other polar aryl groups led to heterocycles, especially 1,3-pyrimidine, which afforded compounds with good potency, low HLM Cl, and modest efflux (MDR BA/AB) as demonstrated in **15** (Figure 9). Unfortunately, in vivo assessment of brain penetration in rat showed a brain/plasma ratio of 0.1 and with C_{bu}/C_{pu} ratio of 0.05, indicative of impaired brain access.

It was surmised that the relatively high TPSA of **15** (111 Å²) could be a factor contributing to the efflux, so we next prepared the less polar cyclopentyl analogue **16** (TPSA = 102 Å²). In this case, improved potency, moderate HLM Cl, high permeability with no P-gp-efflux, and acceptable PDE1C selectivity were observed. Assessment of brain penetration in rat demonstrated a significantly improved brain/plasma ratio of 1.8 and CSF/C_{pu} ratio of 2.2, confirming good brain penetration in vivo. The corresponding CNS MPO score of 5.3/6 indicated that **16** resided in excellent physicochemical property space, in line with the observed in vitro and in vivo ADME properties. Additionally, the strategy of disrupting the phenylpiperidine pharmacophore was clearly successful with human DAT K_i > 10 μM.

On the basis of the favorable results with **16**, it was further evaluated, revealing a significant chemical instability issue in aqueous acidic and neutral systems (pH = 1−6.8). HPLC analysis showed a new peak forming with the same mass as **16**, with a subsequent peak that grew in intensity with mass 18 AMU greater than parent, suggestive of the addition of water. Spectral analysis of a sample of **16** treated with acid was not conclusive due to the presence of overlapping diastereomeric NMR signals, but hydrolytic opening of the azetidine was suggested. To more definitively understand the mechanism of this process, the achiral precursor **17** was treated with aqueous hydrochloric acid (Scheme 4). Clean conversion to a new product with mass 18 AMU higher than the starting material was observed . Spectral analysis (¹H NMR, ¹³C NMR, and IR)

Table 2. SAR of 3-(OAr) Azetidines

Compound	Ar	PDE9A IC$_{50}$ (nM)	HLM Cl (ml/min/kg)	MDR BA/AB	cLogP
10a	F—⬡—ξ	50	27	1.3	0.86
10b	(F, aryl)	57	40	1.4	0.85
10c	(Cl, F, F-aryl)	64	91	1.5	1.1
10d	NC—⬡—ξ	70	<8	2.1	0.3
10e	(NC, F-aryl)	43	<8	2.7	0.5
10f	(NC, Cl-aryl)	19	35	3.1	1.0
10g	(NC, F-aryl)	47	19	4.1	0.5

PDE9A IC$_{50}$ = 63 nM (±)
PDE1C IC$_{50}$ > 1 uM
HLM Cl, int < 7 ml/min/kg
MDR BA/AB = 3

PDE9A IC$_{50}$ = 7 nM
PDE1C IC$_{50}$ = 526 nM
HLM Cl, int = 19 ml/min/kg
MDR BA/AB = 1.3
MDR AB = 18.5 x 10^{-6} cm/sec

Figure 9. Lead analogue 15 and less polar derivative 16.

indicated that 18 was the final product. The mechanism for formation is proposed to proceed via initial protonation of the azetidine nitrogen followed by intramolecular attack of the pyrimidine nitrogen on the azetidine carbon at the 2-position, driven by relief of ring strain. The cyclic pyrimidinium intermediate is subsequently hydrolyzed via attack of water on the 2-position carbon, leading to the observed product. Correspondingly, the phenoxy derivative 7 showed excellent stability in aqueous acid, supporting the key role of the appropriately aligned nucleophilic pyrimidine nitrogen in the reactivity of 16.

To address this issue, we sought to alter the nucleophilic trajectory of the pyrimidine nitrogens toward the azetidine 2-

Scheme 4. Proposed Mechanism for Rearrangement of 17 to 18
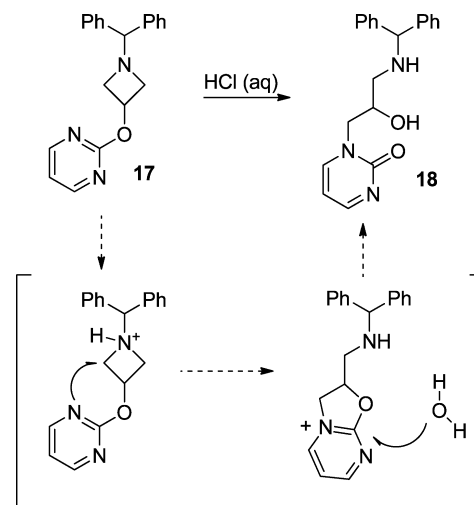
position via removal of the oxygen linker. Docking of 19 (Figure 10) in the PDE9A crystal structure suggested that this structural modification would be tolerated, and results validated this prediction. Indeed, the acid stability of 19 was greatly improved as compared to 16 with no decomposition noted after 10 h at pH < 2. The PDE9A potency of 19 was good (IC$_{50}$ = 32 nM), with acceptable selectivity over PDE1C (30-fold). Examination of the X-ray crystal structure of 19 bound to PDE9A showed a similar binding as previous analogues, except

19
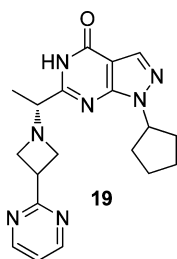
PDE9A IC$_{50}$ = 32 nM	MW = 365
PDE1C IC$_{50}$ = 900 nM	cLogP = -0.4
HLM Cl,int = 15 ml/min/kg	TPSA = 92 A^2
MDR BA/AB = 1	H-bond donor = 1
MDR AB = 22 x 10^{-6} cm/sec	pKa (measured) = 6.8
DAT inib = 0% @ 10 uM	MPO = 5.7/6

Figure 10. Calculated physicochemical properties and in vitro data for **19**.

that removal of the oxygen linker between the pyrimidine and azetidine resulted in a π-stacking interaction between the pyrimidine and Phe441 as opposed to Phe456 (Figure 11).
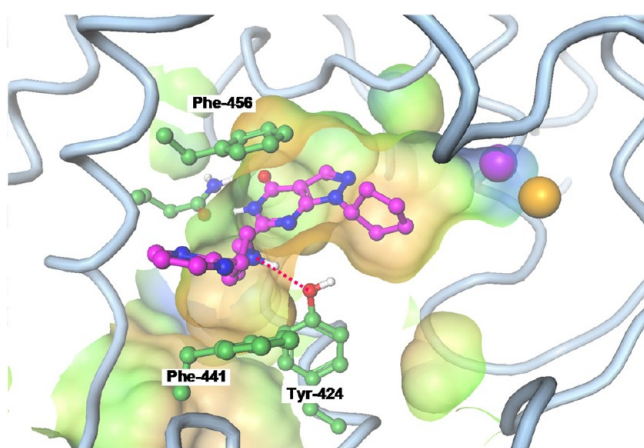

Figure 11. X-ray crystal structure of **19** bound to PDE9A (PDB 4G2L).

Excluding PDE1, no inhibition (≤10% at 1 μM) was observed against all other PDE families and no significant activity was seen against a broad selectivity panel at 10 μM. Microsomal clearance was low and permeability was high with no sign of P-gp-efflux. Physicochemical properties were in highly desirable ranges for **19** with regard to CNS MPO (5.7/6) as well as toxicity.[9] Cytochrome p450 inhibition assays suggested a low likelihood of drug−drug interactions.

Further profiling of **19** in vivo was performed due to its promising in vitro profile. Assessment of rat brain penetration showed a brain/plasma ratio of 1.4 and a C_{bu}/C_{pu} ratio and CSF/C_{pu} ratio of 1.4, indicative of unrestricted CNS access. Oral pharmacokinetics in both rat and dog were favorable with high oral bioavailability, moderate (rat) to low (dog) clearance, and moderate volumes of distribution (Table 3). Predicted human pharmacokinetics based upon microsomal scaling and adjusting for human fraction unbound in plasma (fu$_p$) and microsomes (fu$_{mic}$) suggested high oral bioavailability and moderate to low clearance with with a predicted $T_{1/2}$ of 5 h.[19] Additional in vitro safety profiling included the assessment of hERG channel affinity (IC$_{50}$ = 53.5 μM) that suggested a low

Table 3. Measured Preclinical Pharmacokinetics and Predicted Human Pharmacokinetics of 19

	rat	dog	human (predicted)
% F	63	71	80
Cl (mL/min/kg)	47	6.5	5
V (L/kg)	1.8	1.7	2
T1/2 (h)	1.1	4.4	5

liability for QTC prolongation and a general cellular toxicity assay that showed little toxicity at 300 μM.

In vivo elevation of CSF cGMP in rat with **19** was evaluated to demonstrate a pharmacodynamic response resulting from PDE9A inhibition, which has been previously translated from preclinical to human clinical studies with **2**.[20] Therefore, a solution of **19** was dosed subcutaneously to rats at a dose of 3.2 mg/kg and CSF cGMP and **19** levels were measured over the time period of 30 min to 7 h (Figure 12). A doubling in CSF
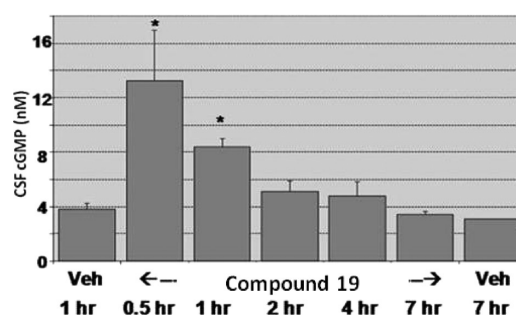
Figure 12. CSF cGMP levels in rats treated with compound **19** as compared to vehicle.

cGMP was observed at one hour, at which point CSF drug levels of **19** were measured to be 389 nM, approximately 10-fold the PDE9A IC$_{50}$. This pharmacodynamic elevation of CSF cGMP aligns with the preclinical response observed with **2**. Therefore, the excellent pharmacokinetics, selectivity, and safety properties of **19** in conjunction with the clearly demonstrated in vivo efficacy led to its nomination as a preclinical candidate.

In summary, a novel series of PDE9A inhibitors was identified via a strategy utilizing structure-based design, parallel chemistry, and physical property optimization. Taking advantage of the synthetically enabled nature of the phenoxy group in **3h**-(R) afforded pyrimidine **16**, which addressed undesired DAT inhibition. Mechanistic understanding of the unexpected chemical instability of **16** was used to prepare the chemically stable compound **19** that met key criteria for HLM Cl, MDR BA/AB, and physical properties (TPSA, clogP), which has been successfully advanced through preclinical in vivo pharmacokinetic, efficacy, and safety studies resulting in its nomination as a preclinical candidate.

■ EXPERIMENTAL SECTION

Biological Data. All compounds were screened in PDE9A inhibition assay as described below. Each IC$_{50}$ value is comprised of at least two measurements of inhibition per data point.

PDE9A IC$_{50}$, 384-well assay: Test compounds were solubilized in 100% dimethyl sulfoxide and diluted to the required concentrations in 15% dimethyl sulfoxide/water. The PDE9A enzyme was thawed slowly and diluted in 50 mM Tris HCl buffer (pH 7.5 at room temperature) containing 1.3 mM MgCl$_2$. Incubations were initiated by the addition of PDE9A enzyme to 384-well plates containing test drugs and

radioligand (50 nM ^{3}H-cGMP). After a 30 min incubation at room temperature, 10 μM 6-benzyl-1-cyclopentyl-1,5-dihydro-4H-pyrazolo-[3,4-d]pyrimidin-4-one was added to each well of the plate to stop the reaction. Phosphodiesterase SPA beads (Amersham/GE) were then added to the assay plate at a concentration of 0.2 mg/well. Activity of test compounds was assessed by measuring the amount of ^{3}H-5′GMP resulting from enzyme cleavage of ^{3}H-cGMP radioligand. Levels of ^{3}H-5′GMP bound to SPA beads were determined by paralux counting of the assay plates in a Microbeta Trilux counter (PerkinElmer). Nonspecific binding was determined by radioligand binding in the presence of a saturating concentration of 6-benzyl-1-cyclopentyl-1,5-dihydro-4H-pyrazolo[3,4-d]pyrimidin-4-one (10 μM). The IC$_{50}$ value of each test compound (concentration at which 50% inhibition of specific binding occurs) was calculated by nonlinear regression (curve fitting) of the concentration−response.

Chemistry Experimentals. Experiments were generally carried out under inert atmosphere (nitrogen or argon), particularly in cases where oxygen- or moisture-sensitive reagents or intermediates were employed. Commercial solvents and reagents were generally used without further purification, including anhydrous solvents where appropriate (generally Sure-Seal products from the Aldrich Chemical Co., Milwaukee, WI). Mass spectrometry data is reported from either liquid chromatography−mass spectrometry (LCMS) or atmospheric pressure chemical ionization (APCI) instrumentation. Chemical shifts for nuclear magnetic resonance (NMR) data are expressed in parts per million (ppm, δ) referenced to residual peaks from the deuterated solvents employed, or to tetramethylsilane standard with multiplicities given as s (singlet), br (broad), d (doublet), t (triplet), dt (doublet of triplets), m (multiplet). Compound purity is determined by high performance liquid chromatography (HPLC), and all final test compounds were >95% purity. The purity of title compounds used in pharmacology testing was verified by HPLC-MS using the following method: 12 min gradient on a HP1100C pump of increasing concentrations of acetonitrile in water (5→95%) containing 0.1% formic acid with a flow rate of 1 mL/min and UV detection at λ 220 and 254 nm on a Gemini C18 150 mm ×4.6 mm, 5 μm column (Phenomenex, Torrance, CA).

5-Amino-1-cyclopentyl-1H-pyrazole-4-carbonitrile (4a). A solution of cyclopentylhydrazine dihydrochloride (50.9 g, 0.294 mol) in anhydrous ethanol (640 mL) was cooled to 0 °C and treated with sodium ethoxide (40.0 g, 0.588 mol) in portions over 2 h. The mixture was stirred at 0 °C for 45 min and then treated dropwise with a solution of (ethoxymethylene)malononitrile (35.9 g, 0.294 mol) in ethanol over 1 h. Following the addition, the reaction was stirred at 0 °C for 30 min and then warmed to room temperature over 1 h. The mixture was heated at reflux for 2 h, cooled to room temperature, and concentrated in vacuo, after which the residue was mixed with water, and the resulting suspension was filtered. The collected solids were washed three times with water and then three times with a 1:1 mixture of diethyl ether and hexanes, providing the titled compound as a beige solid. Yield: 44.0 g, 0.250 mol, 85%. ^{1}H NMR (400 MHz, CDCl$_3$) δ 1.69 (m, 2H), 1.92 (m, 2H), 2.06 (m, 4H), 4.34 (m, 1H), 7.50 (s, 1H).

5-Amino-1-cyclopentyl-1H-pyrazole-4-carboxamide (5a). 5-Amino-1-cyclopentyl-1H-pyrazole-4-carbonitrile (44.0 g, 0.250 mol) was added portionwise to concentrated sulfuric acid (200 mL) at 0 °C. After completion of the addition, the reaction mixture was allowed to warm from 0 °C to room temperature and stirred for about 18 h. The reaction mixture was poured onto ice and then brought to pH 9−10 by addition of concentrated aqueous ammonium hydroxide solution. The resulting solids were collected by filtration, washed three times with water, and then washed three times with a 1:1 mixture of diethyl ether and hexanes to provide 5a as an off-white solid. Yield: 39.8 g, 0.205 mol, 82%. LCMS m/z 195.4 (M + 1). ^{1}H NMR (400 MHz, DMSO-d_6) δ 1.57 (m, 2H), 1.80 (m, 4H), 1.92 (m, 2H), 4.52 (m, 1H), 6.15 (s, 2H), 6.61 (br s, 1H), 7.15 (br s, 1H), 7.62 (s, 1H).

6-(1-Bromoethyl)-1-cyclopentyl-1,5-dihydro-4H-pyrazolo[3,4-d]-pyrimidin-4-one (6a). A solution of 5a (5.0 g, 25.8 mmol) and triethylamine (4.0 mL, 28.4 mmol) in anhydrous dimethylformamide (50 mL) was cooled in an ice bath and treated dropwise with 2-bromopropanoyl bromide (2.8 mL, 28.4 mmol). The mixture was

stirred at 0 °C for 20 min, warmed to room temperature, and stirred at ambient temperature for an additional 2 h. The reaction mixture was diluted with ethyl acetate (500 mL) and washed sequentially with aqueous 3N hydrochloric acid (3 × 300 mL; then 2 × 50 mL), saturated aqueous sodium bicarbonate solution (2 × 300 mL), and saturated aqueous sodium chloride solution (300 mL). The organic layer was dried over magnesium sulfate, filtered, and concentrated. The resulting crude residue was stirred as a suspension in toluene (200 mL) with *para*-toluenesulfonic acid (2.45 g, 12.9 mmol), and the mixture was heated to reflux for 4 h using a Dean−Stark trap. The mixture was then cooled to room temperature, diluted with ethyl acetate, and washed with aqueous sodium bicarbonate solution followed by saturated aqueous sodium chloride solution. The organic layer was dried over magnesium sulfate, filtered, and concentrated to provide a residue that was purified by silica gel chromatography (eluant: 100:1 chloroform/methanol). The resulting yellow−orange solid was subjected to a second silica gel column (eluant 100:1 chloroform/methanol) to provide 1.8 g (22%) of 6 as a solid. LCMS m/z 311, 313 for the two bromine isotopes (M + 1). [α]$_D$ = −32.1 (c 0.005 g/mL, MeOH). ^{1}H NMR (400 MHz, CDCl$_3$) δ 1.60−2.24 (m, 8H), 2.11 (d, J = 7.0 Hz, 3H), 5.04 (q, J = 7.0, 1H), 5.20 (quintet, J = 7.5 Hz, 1H), 8.10 (s, 1H), 11.85 (br s, 1H).

Library Preparation of N-Substituted 6-(1-Aminoethyl)-1-cyclopentyl-1,5-dihydro-4H-pyrazolo[3,4-d]pyrimidin-4-ones (3). The amines (0.14 mmol) were weighed into vials and treated with a solution of 6a (22 mg, 0.07 mmol) in a 1:5 mixture of dimethylformamide/acetonitrile (0.6 mL). Potassium carbonate (29 mg, 0.21 mmol) was added, and the reactions were shaken and heated at 82 °C for 8 h. The reactions were then cooled to room temperature, and water (1.5 mL) and ethyl acetate (2.5 mL) were added. After vortexing the reactions, the organic portions were separated and passed through a short column of sodium sulfate. This process was repeated two times. The combined filtrates for each reaction were concentrated in vacuo and then treated with a 3% solution of trifluoroacetic acid in dichloromethane (0.5 mL). The mixtures were shaken for 15 min, solvent was removed in vacuo, and the crude samples were dissolved in dimethyl sulfoxide (1 mL) and purified by preparative HPLC (column: Xterra PrepMS C$_{18}$, 5 μm, 19 mm × 100 mm; solvent A, 0.1% trifluoroacetic acid in water (v/v); solvent B, acetonitrile; gradient, 5% to 95% B), to afford the final examples 3 as trifluoroacetic acid salts (Table 4).

Table 4

	exact mass	MS (obsd)	% ELSD purity	% UV purity (220 nM)	retention time (min)	amount (mg)
3a	315.21	316.37	100	100	2.65	18.2
3b	319.18	320.16	100	100	2.49	21
3c	287.15	288.24	100	100	2.41	19
3d	397.17	398.09	100	93	3.08	22.4
3e	405.25	406.18	100	93	3.23	22.9
3f	377.22	378.23	100	100	2.98	21.1
3g	423.23	424.21	100	85	2.96	26.3
3h	379.20	380.29	100	94	2.99	17.8

1-Cyclopentyl-6-[(1R)-1-(3-phenoxyazetidin-1-yl)ethyl]-1,5-dihydro-4H-pyrazolo[3,4-d]pyrimidin-4-one (3h-(R)). A mixture of 6a (400 mg, 1.29 mmol), 3-hydroxyazetidine hydrochloride (479 mg, 2.58 mmol), and potassium carbonate (534 mg, 3.87 mmol) in acetonitrile (15 mL) was stirred at room temp for 2 h and then refluxed for 2 h. The reaction mixture was cooled, diluted with water, and extracted with methylene chloride. The organic layer was washed with brine, dried over magnesium sulfate, filtered, concentrated, and chromatographed (eluant: 1:1 ethyl acetate/hexanes with 1% ammonium hydroxide) to provide 240 mg of 3h as a solid. Chiral separation of racemate 3h was performed using the following conditions: Chiralcel OD, 10 cm × 50 cm, 250 mL/min; eluant 65:35 heptane/ethanol. The undesired enantiomer was isolated first

and provided 111 mg of solid. The second enantiomer was isolated with a retention time of 26 min and provided 82 mg of the desired enantiomer **3h**-(*R*) solid. LCMS *m/z* 380.0 (M + 1). ^{1}H NMR (400 MHz, CDCl$_3$) δ 1.35 (d, 3H, *J* = 6.6), 1.65−1.68 (m, 2H), 1.92−2.08 (m, 2H), 2.08−2.15 (m, 4H), 3.24 (br s, 1H), 3.38−3.42 (br m, 1H), 3.57 (br s, 1H), 3.88 (br s, 1H), 4.80−4.86 (m, 1H), 5.12−5.19 (m, 1H), 6.76 (d, 2H, *J* = 7.9), 6.95−6.99 (m, 1H), 7.25−7.29 (m, 2H), 8.05 (s, 1H), 9.78 (br s, 1H). ^{13}C NMR (100 MHz, CDCl$_3$) δ 18.07, 24.72, 32.39, 32.45, 57.77, 58.77, 60.49, 65.23, 65.55, 105.08, 114.55, 121.47, 129.67, 134.57, 151.98, 156.69, 157.93.

5-Amino-1-(tetrahydro-2H-pyran-4-yl)-1H-pyrazole-4-carbonitrile (4b). To a solution of tetrahydro-2*H*-pyran-4-ylhydrazine dihydrochloride (see ref 21) (43 g, 228 mmol) in ethanol (300 mL) was slowly added sodium ethoxide (32.6 g, 479 mmol), and the resulting mixture was stirred at room temperature for 1 h. The reaction mixture was then transferred into a solution of (ethoxymethylene)-malononitrile (27.8 g, 228 mmol) in ethanol (300 mL). After being stirred at room temperature for 30 min, the reaction was heated at reflux for 2 h. It was then cooled to room temperature and concentrated in vacuo to afford the titled compound as an orange solid, which was used in the next step without purification.

5-Amino-1-(tetrahydro-2H-pyran-4-yl)-1H-pyrazole-4-carboxa-mide (5b). A solution of 5-amino-1-(tetrahydro-2*H*-pyrazole-4-carbonitrile (**4b**, ≤228 mmol) in ethanol (300 mL) was treated with 35% aqueous hydrogen peroxide (100 mL), followed by concentrated aqueous ammonia solution (300 mL). The reaction mixture was stirred for 48 h at room temperature and then quenched with saturated aqueous sodium thiosulfate solution (800 mL). Removal of most of the ethanol in vacuo provided a solid that was isolated by filtration and washed with water (2 × 200 mL) and diethyl ether (2 × 150 mL) to provide **5b** as a solid. Yield: 31 g, 147 mmol, 64% for 2 steps. LCMS *m/z* 211.2 (M + 1). ^{1}H NMR (300 MHz, DMSO-*d$_6$*) δ 1.70 (m, 2H), 1.93 (m, 2H), 3.40 (m, 2H), 3.95 (dd, *J* = 11.1, 3.2 Hz, 2H), 4.26 (m, 1H), 6.24 (m, 2H), 6.67 (br s, 1H), 7.20 (br s, 1H), 7.66 (s, 1H).

6-(1-Bromoethyl)-1-(tetrahydro-2H-pyran-4-yl)-1,5-dihydro-4H-pyrazolo[3,4-d]pyrimidin-4-one (6b). A solution of **5b** (5.0 g, 23.8 mmol) and triethylamine (3.65 mL, 26.2 mmol) in anhydrous dimethylformamide (50 mL) was cooled in an ice bath and treated dropwise with 2-bromopropanoyl bromide (5.4 g, 25 mmol). The mixture was stirred at 0 °C for 30 min, warmed to room temperature, and stirred at ambient temperature for an additional 2 h. The reaction was partitioned between ethyl acetate (200 mL) and aqueous 2N hydrochloric acid (500 mL); the organic phase was washed with saturated aqueous sodium bicarbonate solution (400 mL), followed by saturated aqueous sodium chloride solution (200 mL) and then dried over sodium sulfate, filtered, and concentrated. The resulting orange residue was suspended in toluene (100 mL), treated with *para*-toluenesulfonic acid (2.3 g, 11.9 mmol), and heated to reflux for 6 h using a Dean−Stark trap. The mixture was then cooled to room temperature, diluted with ethyl acetate, and washed with aqueous sodium bicarbonate solution, followed by saturated aqueous sodium chloride solution. The organic layer was dried over sodium sulfate, filtered, and concentrated in vacuo to provide a residue that was purified by silica gel chromatography (eluant: 100:1 chloroform/methanol). The resulting yellow−orange solid was subjected to a second silica gel column (eluant 100:1 chloroform/methanol) to provide the titled compound as a yellow solid. Yield: 1.1 g, 3.36 mmol, 14% over two steps. Purity: 85% by LCMS. LCMS *m/z* 327.0, 329.1 for the two bromine isotopes (M + 1). ^{1}H NMR (400 MHz, CD$_3$OD) δ 1.92 (m, 2H), 2.06 (d, *J* = 6.3 Hz, 3H), 2.31 (m, 2H), 3.63 (m, 2H), 4.08 (m, 2H), 4.94 (m, 1H), 5.09 (q, *J* = 6.6 Hz, 1H), 8.05 (s, 1H).

6-[1-(3-Hydroxyazetidin-1-yl)ethyl]-1-(tetrahydro-2H-pyran-4-yl)-1,5-dihydro-4H-pyrazolo[3,4-d]pyrimidin-4-one (8). A solution of *tert*-butyl 3-hydroxyazetidine-1-carboxylate (519 mg, 3.00 mmol) in dichloromethane (10 mL) was treated with trifluoroacetic acid (0.77 mL, 10 mmol), and the resulting mixture was stirred at room temperature for about 18 h. Additional trifluoroacetic acid (0.5 mL) was added, and the reaction was stirred for an additional 3 h. Solvents were removed under reduced pressure, and acetonitrile (40 mL) was

added to the residue, followed by solid potassium carbonate (2.76 g, 20 mmol) and 6-(1-bromoethyl)-1-(tetrahydro-2*H*-pyran-4-yl)-1,5-dihydro-4*H*-pyrazolo[3,4-*d*]pyrimidin-4-one (**6b**, 654 mg, 2.00 mmol). The mixture was stirred at room temperature for 2 h and then heated to 90 °C for 3 h. The reaction was cooled to room temperature, diluted with dichloromethane, and filtered; the remaining solid was washed with additional dichloromethane. The combined filtrates were concentrated in vacuo and then subjected to silica gel chromatography (eluant: 40:1 to 20:1 chloroform/methanol) to provide the titled compound **8b** (368 mg, 58%). MS (APCI) *m/z* 320.0 (M + 1). ^{1}H NMR (400 MHz, CDCl$_3$) δ 1.34 (d, *J* = 6.8 Hz, 3H), 1.91 (m, 2H), 2.38 (dddd, apparent qd, *J* = 12, 12, 12, 4.6 Hz, 2H), 3.17 (br s, 1H), 3.28 (br s, 1H), 3.52−3.68 (m, 5H), 4.14 (dd, *J* = 11.3, 3.6 Hz, 2H), 4.46 (m, 1H), 4.85 (tt, *J* = 11.6, 4.2 Hz, 1H), 8.10 (s, 1H).

1-{1-[4-Oxo-1-(tetrahydro-2H-pyran-4-yl)-4,5-dihydro-1H-pyrazolo[3,4-d]pyrimidin-6-yl]ethyl}azetidin-3-yl Methanesulfonate (9). A solution of **8** (1.34 g, 4.20 mmol) in dichloromethane (30 mL) was treated with triethylamine (1.17 mL, 8.41 mmol) and then dropwise with methanesulfonyl chloride (0.49 mL, 6.3 mmol). The reaction was allowed to stir at room temperature for about 18 h, then saturated aqueous sodium carbonate solution was added, and the aqueous layer was extracted twice with dichloromethane. The combined organic layers were dried over magnesium sulfate, filtered, and concentrated. The residue was purified twice by silica gel chromatography (gradient, 0−4% methanol in dichloromethane), to afford the titled compound **9** as a solid (1.12 g, 67%). LCMS *m/z* 398.3 (M + 1). ^{1}H NMR (400 MHz, CD$_3$OD) δ 1.36 (d, *J* = 6.6 Hz, 3H), 1.90 (m, 2H), 2.29 (m, 2H), 3.10 (s, 3H), 3.39 (dd, *J* = 8.3, 5.4 Hz, 1H), 3.44 (dd, *J* = 8.4, 5.3 Hz, 1H), 3.62 (m, 3H), 3.76 (br dd, *J* = 7.4, 7.4 Hz, 1H), 3.84 (br dd, *J* = 7.4, 7.4 Hz, 1H), 4.10 (br d, *J* = 11.6 Hz, 2H), 4.97 (tt, *J* = 11.6, 4.2 Hz, 1H), 5.15 (m, 1H), 8.03 (s, 1H).

1-Cyclopentyl-6-[(1S)-1-hydroxyethyl]-1,5-dihydro-4H-pyrazolo-[3,4-d]pyrimidin-4-one (11a). (1*S*)-2-Chloro-1-methyl-2-oxoethyl acetate (12 mL, 95 mmol) was slowly added dropwise to an ice-cooled suspension of **5a** (16.4 g, 84.4 mmol) in anhydrous 1,4-dioxane (200 mL). After being stirred at 0 °C for 40 min, the reaction mixture was heated at reflux for 2 h. It was then cooled to room temperature and concentrated in vacuo, and the resulting crude material was dissolved in a mixture of water (200 mL) and tetrahydrofuran (20 mL). To this solution was added potassium carbonate (60 g, 0.43 mol), and the resulting mixture was heated at 50 °C for 2 days. The reaction mixture was cooled to room temperature and extracted with ethyl acetate (2 × 200 mL). The combined organic extracts were washed with saturated aqueous sodium chloride solution, dried over sodium sulfate, filtered, and concentrated in vacuo to provide **11a** as a tan solid. Yield: 17.5 g, 70.5 mmol, 84% over 2 steps. LCMS *m/z* 249.4 (M + 1). ^{1}H NMR (400 MHz, DMSO-*d$_6$*) δ 1.41 (d, *J* = 6.6 Hz, 3H), 1.67 (m, 2H), 1.90 (m, 4H), 2.06 (m, 2H), 4.61 (q, *J* = 6.6 Hz, 1H), 5.13 (m, 1H), 8.02 (s, 1H).

(1S)-1-(1-Cyclopentyl-4-oxo-4,5-dihydro-1H-pyrazolo[3,4-d]-pyrimidin-6-yl)ethyl Methanesulfonate (12a). A solution of **11a** (93% purity by weight, 87.7 g, 329 mmol) in 2-methyltetrahydrofuran (408 mL) was treated with 4-methylmorpholine (54.4 mL, 495 mmol), followed, after 5 min, by methanesulfonyl chloride (26.7 mL, 345 mmol). The temperature of the reaction was maintained between 25 and 40 °C for 3 h. After cooling to room temperature, the reaction mixture was filtered through Celite to remove morpholine salts, and the filter cake was washed with 5−10 volumes of 2-methyltetrahydrofuran. The filtrate was concentrated in vacuo and then purified by silica gel chromatography (eluant: 9:1 ethyl acetate/hexanes). Pure fractions were combined and concentrated to afford **9a** as a slightly yellow solid. Yield: 48.6 g, 149 mmol, 45%. Mixed fractions were combined and concentrated to provide 40 g of a residue which was purified by trituration with methyl *tert*-butyl ether (100 mL) to provide additional **9a** as a white solid. Combined yield: 79.5 g, 244 mmol, 74%. LCMS *m/z* 325.1 (M − 1). ^{1}H NMR (400 MHz, CDCl$_3$) δ 1.75 (m, 2H), 1.86 (d, *J* = 6.8 Hz, 3H), 1.99 (m, 2H), 2.13 (m, 4H), 3.23 (s, 3H), 5.18 (m, 1H), 5.70 (q, *J* = 6.7 Hz, 1H), 8.07 (s, 1H), 11.04 (br s, 1H).

6-[(1S)-1-Hydroxyethyl]-1-(tetrahydro-2H-pyran-4-yl)-1,5-dihydro-4H-pyrazolo[3,4-d]pyrimidin-4-one (11b). (1S)-2-Chloro-1-methyl-2-oxoethyl acetate (30 g, 199 mmol) was added to a suspension of **5b** (38.1 g, 181 mmol) in dry dioxane (1000 mL). The mixture was heated at reflux for 2 h amd then concentrated in vacuo to provide (1S)-2-{[4-carbamoyl-1-(tetrahydro-2H-pyran-4-yl)-1H-pyrazol-5-yl]amino}-1-methyl-2-oxoethyl acetate, which was suspended in water (700 mL) and treated with anhydrous potassium carbonate (100 g). The mixture was heated at 45 °C for about 18 h and then neutralized with acetic acid and extracted with chloroform (4 × 1 L). The combined organic layers were washed with saturated aqueous sodium chloride solution and dried over sodium sulfate. Filtration and removal of solvents in vacuo provided **11b** as an off-white solid. Yield: 43.1 g, 163 mmol, 90% over 2 steps. LCMS m/z 265.2 (M + 1). ^{1}H NMR (400 MHz, CDCl$_3$) δ 1.67 (d, J = 6.6 Hz, 3H), 1.92 (br d, J = 13 Hz, 2H), 2.39 (m, 2H), 3.62 (br dd, apparent br t, J = 12, 12 Hz, 2H), 4.15 (br dd, J = 11.7, 4 Hz, 2H), 4.84 (tt, J = 11.6, 4.3 Hz, 1H), 4.90 (q, J = 6.7 Hz, 1H), 8.08 (s, 1H), 10.65 (br s, 1H).

(1S)-1-[4-Oxo-1-(tetrahydro-2H-pyran-4-yl)-4,5-dihydro-1H-pyrazolo[3,4-d]pyrimidin-6-yl]ethyl Methanesulfonate (12b). A solution of **11b** (20.0 g, 75.7 mmol) in dichloromethane (400 mL) was treated with triethylamine (15.8 mL, 113 mmol), cooled to 0 °C, and stirred for 30 min. Methanesulfonyl chloride (99%, 5.92 mL, 75.7 mmol) was added dropwise to the cold reaction, which was allowed to warm to room temperature over the next 18 h. Solvents were removed in vacuo, and the residue was purified by silica gel chromatography (gradient 0–5% methanol in dichloromethane). Rechromatography of mixed fractions provided additional product to afford **12b** as a solid. Total yield: 10.6 g, 31.0 mmol, 41%. LCMS m/z 341.1 (M − 1). ^{1}H NMR (400 MHz, CDCl$_3$) δ 1.86 (d, J = 6.6 Hz, 3H), 1.93 (br d, J = 12 Hz, 2H), 2.39 (m, 2H), 3.23 (s, 3H), 3.61 (ddd, apparent td, J = 12, 12, 2.1 Hz, 2H), 4.16 (br dd, J = 11.4, 3.5 Hz, 2H), 4.86 (tt, J = 11.7, 4.2 Hz, 1H), 5.70 (q, J = 6.7 Hz, 1H), 8.08 (s, 1H).

6-[(1R)-1-(3-Phenoxyazetidin-1-yl)ethyl]-1-(tetrahydro-2H-pyran-4-yl)-1,5-dihydro-4H-pyrazolo[3,4-d]pyrimidin-4-one (7). Step 1: 3-Phenoxyazetidine. Commercial 3-phenoxyazetidine hydrochloride (5.57 g, 30.0 mmol) and sodium hydroxide (1.44 g, 36.0 mmol) were stirred at room temperature in dichloromethane (150 mL) and water (50 mL). The mixture was stirred at room temperature for 5 h. The organic layer was separated, and the water layer was extracted with dichloromethane. The combined organic phases were dried over MgSO$_4$, filtered, and concentrated to give 4.4 g of 3-phenoxyazetidine as the free base, which was used without further purification.

Step 2: 6-[(1R)-1-(3-Phenoxyazetidin-1-yl)ethyl]-1-(tetrahydro-2H-pyran-4-yl)-1,5-dihydro-4H-pyrazolo[3,4-d]pyrimidin-4-one, (7). Mesylate **12b** (4.6 g, 13.4 mmol) and 3-phenoxyazetidine (3.01 g, 20.2 mmol) were combined with triethylamine (9.36 mL, 67.2 mmol), acetonitrile (50 mL), and toluene (50 mL). The mixture was heated at 90 °C for 5 h with stirring and then concentrated. The residue was purified by silica gel chromatography (1% methanol in chloroform) to provide 4.93 g (93% yield) of **9** as a solid. LCMS m/z 396.4 (M + 1). ^{1}H NMR (400 MHz, CDCl$_3$) δ 1.38 (d, J = 6.8 Hz, 3H), 1.89 (m, 2H), 2.29 (m, 2H), 3.28 (dd, assumed, partially obscured by solvent peak, J = 8.1, 5.2 Hz, 1H), 3.34 (dd, assumed, partially obscured by solvent peak, J = 7.9, 5.4 Hz, 1H), 3.61 (m, 3H), 3.85 (dd, J = 7.0, 7.0 Hz, 1H), 3.93 (dd, J = 6.9, 6.9 Hz, 1H), 4.08 (m, 2H), 4.87 (m, 1H), 4.98 (tt, J = 11.7, 4.2 Hz, 1H), 6.80 (d, J = 8.2 Hz, 2H), 6.93 (t, J = 7.8 Hz, 1H), 7.26 (dd, J = 7.8, 7.8 Hz, 2H), 8.03 (s, 1H).

1-Cyclopentyl-6-{(1R)-1-(3-hydroxyazetidin-1-yl)ethyl}-1,5-dihydro-4H-pyrazolo[3,4-d]pyrimidin-4-one (13a). N-Boc-3-hydroxyazetidine (2.50 g, 14.4 mmol) was treated with trifluoroacetic acid (3.7 mL) in dichloromethane (20 mL). The mixture was stirred at room temperature overnight and then concentrated. To the resulting residue was added acetonitrile (20 mL) and toluene (20 mL), followed by potassium carbonate (finely ground, 13.3 g, 96.0 mmol). Mesylate **12a** (3.13 g, 9.60 mmol) was then added, and the mixture was heated to 90 °C for 5 h with stirring. The mixture was concentrated to remove all solvents, diluted with water, and extracted with methylene chloride. The combined extracts were washed with brine, dried over MgSO$_4$,

filtered, concentrated, and chromatographed (eluant 50:1 CHCl$_3$/CH$_3$OH) to give 2.0 g of **13a**. LCMS m/z 304.4 (M + 1). ^{1}H NMR (400 MHz, CDCl$_3$) δ 1.31 (d, 3H, J = 6.6), 1.64–1.74 (m, 2H), 1.90–2.15 (m, 6H), 3.14–3.17 (br m, 1H), 3.25–3.27 (br m, 1H), 3.48–3.62 (m, 3H), 4.39–4.44 (m, 1H), 5.15 (apparent quintet, 1H, J = 7.6), 8.08 (s, 1H).

6-[(1R)-1-(3-Hydroxyazetidin-1-yl)ethyl]-1-(tetrahydro-2H-pyran-4-yl)-1,5-dihydro-4H-pyrazolo[3,4-d]pyrimidin-4-one (13b). The title compound was prepared in a manner analogous to **13a** with the substitution of starting material **12b** in place of **12a** to afford 1.6 g (72% yield) of **13b**. MS (APCI) m/z 320.0 (M + 1). ^{1}H NMR (400 MHz, CDCl$_3$) δ 1.34 (d, J = 6.8 Hz, 3H), 1.91 (m, 2H), 2.38 (dddd, apparent qd, J = 12, 12, 12, 4.6 Hz, 2H), 3.17 (br s, 1H), 3.28 (br s, 1H), 3.52–3.68 (m, 5H), 4.14 (dd, J = 11.3, 3.6 Hz, 2H), 4.46 (m, 1H), 4.85 (tt, J = 11.6, 4.2 Hz, 1H), 8.10 (s, 1H).

(R)-1-{1-[4-Oxo-1-(tetrahydro-2H-pyran-4-yl)-4,5-dihydro-1H-pyrazolo[3,4-d]pyrimidin-6-yl]ethyl}azetidin-3-yl methanesulfonate, (14b). The title compound was prepared in a manner analogous to that of **9** to afford 1.72 g (77% yield) of **14b**. LCMS m/z 398.3 (M + 1). ^{1}H NMR (400 MHz, CD$_3$OD) δ 1.36 (d, J = 6.6 Hz, 3H), 1.90 (m, 2H), 2.29 (m, 2H), 3.10 (s, 3H), 3.39 (dd, J = 8.3, 5.4 Hz, 1H), 3.44 (dd, J = 8.4, 5.3 Hz, 1H), 3.62 (m, 3H), 3.76 (br dd, J = 7.4, 7.4 Hz, 1H), 3.84 (br dd, J = 7.4, 7.4 Hz, 1H), 4.10 (br d, J = 11.6 Hz, 2H), 4.97 (tt, J = 11.6, 4.2 Hz, 1H), 5.15 (m, 1H), 8.03 (s, 1H).

6-{1-[3-(4-Fluorophenoxy)azetidin-1-yl]ethyl}-1-(tetrahydro-2H-pyran-4-yl)-1,5-dihydro-4H-pyrazolo[3,4-d]pyrimidin-4-one (10a). Step 1: 3-(4-Fluorophenoxy)azetidine. Palladium hydroxide (500 mg) and 1-(diphenylmethyl)-3-(4-fluorophenoxy)azetidine (500 mg, 1.50 mmol) were combined in ethanol (50 mL) and hydrogenated at 50 psi for 18 h. The reaction mixture was then filtered through Celite and concentrated in vacuo. The residue was purified via silica gel chromatography (eluant 100:5:2 chloroform/methanol/concentrated aqueous ammonium hydroxide) to provide titled compound (188 mg, 75%). LCMS m/z 168.1 (M + 1). ^{1}H NMR (400 MHz, CDCl$_3$) δ 2.44 (br s, 1H), 3.76 (m, 2H), 3.89 (m, 2H), 4.91 (m, 1H), 6.66 (m, 2H), 6.93 (m, 2H). ^{13}C NMR (100 MHz, CDCl$_3$) δ 54.55, 70.81, 115.43, 115.51, 115.76, 115.99, 152.96, 156.15, 158.53.

Step 2: 6-{1-[3-(4-Fluorophenoxy)azetidin-1-yl]ethyl}-1-(tetrahydro-2H-pyran-4-yl)-1,5-dihydro-4H-pyrazolo[3,4-d]pyrimidin-4-one, (10a). A mixture of 6-(1-bromoethyl)-1-(tetrahydro-2H-pyran-4-yl)-1,5-dihydro-4H-pyrazolo[3,4-d]pyrimidin-4-one (**6b**, 100 mg/0.306 mmol), 3-(4-fluorophenoxy)azetidine (102 mg/0.611 mmol), and potassium carbonate (92.9 mg/0.672 mmol) in acetonitrile (10 mL) was stirred at room temperature for 2 h and refluxed overnight. The mixture was cooled, concentrated, diluted with brine (25 mL) and 1N NaOH (25 mL), and extracted with CH$_2$Cl$_2$. The combined extracts were concentrated, dissolved in DMSO (3.0 mL), and filtered through an Acrodisc syringe filter (0.2 um). The filtrate was concentrated and purified with a Shimadzu HPLC (Xterra 30 mm × 100 mm; 30–70% water/acetonitrile gradient elution with 0.1% NH$_4$OH). The resulting material was further purified by dissolving it in MeOH (3 mL) and passing through an Oasis MCX LP extraction cartridge (1 g) with MeOH, and then the product was eluted with ammonia in MeOH and concentrated to provide 29 mg of **10a**. LCMS m/z 414.4 (M + 1). ^{1}H NMR (400 MHz, CDCl$_3$) δ 1.36 (d, J = 6.6 Hz, 3H), 1.91 (br d, J = 12.6 Hz, 2H), 2.37 (m, 2H), 3.23 (br s, 1H), 3.40 (m, 1H), 3.61 (m, 3H), 3.88 (br s, 2H), 4.14 (dd, J = 11.5, 4.0 Hz, 2H), 4.75–4.88 (m, 2H), 6.71 (m, 2H), 6.97 (m, 2H), 8.06 (s, 1H).

4-[(1-{1-[4-Oxo-1-(tetrahydro-2H-pyran-4-yl)-4,5-dihydro-1H-pyrazolo[3,4-d]pyrimidin-6-yl]ethyl}azetidin-3-yl)oxy]benzonitrile (10d). Step 1: 1-(Diphenylmethyl)azetidin-3-ol Hydrochloride. A solution of 2-(chloromethyl)oxirane (260 g, 2.81 mol) and diphenylmethanamine (500 g, 2.73 mol) in MeOH (1 L) was heated at reflux for 4 days. Solvent was removed under reduced pressure to provide a white precipitate, which was collected by filtration. The solid was washed with acetone and dried to provide title compound, which was used in the next step without further purification.

Step 2: 1-(Diphenylmethyl)azetidin-3-yl Methanesulfonate. Methanesulfonyl chloride (180 g, 1.57 mol) was added to a solution of 1-(diphenylmethyl)azetidin-3-ol hydrochloride (360 g, 1.31 mol) and triethylamine (330 g, 3.26 mol) in dichloromethane (3 L) at 0 °C.

The reaction mixture was stirred at room temperature for 3 h, quenched with saturated aqueous sodium bicarbonate solution, and then extracted with dichloromethane. The combined organic layers were dried over anhydrous sodium sulfate, filtered, and concentrated in vacuo to afford 360 g (87%) of the titled compound.

Step 3: 4-((1-Benzhydrylazetidin-3-yl)oxy)benzonitrile. A mixture of 4-hydroxybenzonitrile (51.5 g, 0.432 mol) and potassium carbonate (120 g, 0.868 mol) in acetonitrile (1.5 L) was refluxed for 1 h. The mixture was cooled, and a solution of 1-(diphenylmethyl)azetidin-3-yl methanesulfonate (124.6 g, 0.392 mol) in acetonitrile (500 mL) was added. The mixture was refluxed for 20 h, cooled to room temperature, poured onto water (2 L), and extracted with ethyl acetate (4 × 700 mL). The combined extracts were washed with 10% aq NaOH (3 × 500 mL), water (500 mL), and brine (100 mL). The organic layer was dried over magnesium sulfate, filtered, and concentrated. The resulting cream-colored solid was shaken with diethyl ether (200 mL) and filtered, rinsing with 1:1 diethyl ether/hexanes (20 mL). After air drying for 2 h, the titled compound was afforded as a white solid (93.1 g, 69.8%).

Step 4: 4-(Azetidin-3-yloxy)benzonitrile Hydrochloride. To a solution of 4-((1-benzhydrylazetidin-3-yl)oxy)benzonitrile (80 g, 0.235 mol) in 1,2-dichloroethane (1 L) at −5 °C was added 1-chloroethyl chloroformate (25.4 mL, 0.235 mol) over 15 min while maintaining the temperature. The reaction mixture was stirred for 15 min at −5 °C, 1 h at room temperature and 1 h at reflux. The mixture was concentrated, dissolved in methanol (1 L), heated to reflux for 2.5 h, and concentrated to approximately 500 mL. Ethyl acetate (500 mL) was added, and the mixture again concentrated to almost 500 mL. Ethyl acetate (500 mL) was again added, and the resulting suspension was stirred for 20 h and then filtered. The resulting solid was dried to afford 34.9 g (70.5%) of the titled compound as a white solid (mp 88−90 °C).

Step 5: 4-[(1-{1-[4-Oxo-1-(tetrahydro-2H-pyran-4-yl)-4,5-dihydro-1H-pyrazolo[3,4-d]pyrimidin-6-yl]ethyl}azetidin-3-yl)oxy]-benzonitrile (10d). A mixture of 6-(1-bromoethyl)-1-(tetrahydro-2*H*-pyran-4-yl)-1,5-dihydro-4*H*-pyrazolo[3,4-*d*]pyrimidin-4-one (**6b**, 100 mg/0.306 mmol), 4-(azetidin-3-yloxy)benzonitrile hydrochloride (65 mg/0.32 mmol), and potassium carbonate (50.7 mg/0.367 mmol) in acetonitrile (10 mL) was stirred at room temperature for 2 h and refluxed for 3 h. Triethylamine (0.085 mL, 0.61 mmol) was added, and the mixture was refluxed overnight. The mixture was cooled, concentrated, diluted with brine (25 mL) and 1N NaOH (25 mL), and extracted with CH₂Cl₂. The combined extracts were concentrated, dissolved in DMSO (3.0 mL), and filtered through an Acrodisc syringe filter (0.2 um). The filtrate was concentrated and purified with a Shimadzu HPLC (Xterra 30 × 100 mm; 30 − 70% water/acetonitrile gradient elution with 0.1% NH₄OH). The resulting material was further purified by dissolving it in MeOH (3 mL) and passing through an Oasis MCX LP extraction cartridge (1 g) with MeOH, and then the product was eluted with ammonia in MeOH and concentrated to provide 12 mg of **10f**. LCMS *m/z* 421.5 (M + 1). ¹H NMR (400 MHz, CD₃OD) δ 1.38 (d, *J* = 6.6 Hz, 3H), 1.89 (m, 2H), 2.29 (m, 2H), 3.30 (m, 1H, assumed, obscured by solvent peak), 3.37 (dd, *J* = 8.1, 5.2 Hz, 1H), 3.61 (m, 3H), 3.88 (dd, *J* = 7.0, 7.0 Hz, 1H), 3.94 (dd, *J* = 7.1, 7.1 Hz, 1H), 4.09 (m, 2H), 4.97 (m, 2H), 6.98 (d, *J* = 8.7 Hz, 2H), 7.65 (d, *J* = 8.7 Hz, 2H), 8.03 (s, 1H).

2-Fluoro-5-[(1-{1-[4-oxo-1-(tetrahydro-2H-pyran-4-yl)-4,5-dihydro-1H-pyrazolo[3,4-d]pyrimidin-6-yl]ethyl}azetidin-3-yl)oxy]-benzonitrile (10g). Mesylate **14b** (50 mg, 0.13 mmol), 2-fluoro-5-hydroxybenzonitrile (34.5 mg, 0.25 mmol), and potassium carbonate (52.2 mg, 0.38 mmol) were combined in acetonitrile (5 mL), and the mixture was heated at reflux for about 18 h. Removal of solvents in vacuo provided a residue which was purified by silica gel chromatography (gradient 1−3% methanol in dichloromethane) to provide **10g** as a solid (19 mg, 33%). LCMS *m/z* 439.3 (M + 1). ¹H NMR (400 MHz, CD₃OD) δ 1.37 (d, *J* = 6.6 Hz, 3H), 1.89 (m, 2H), 2.29 (dddd, *J* = 12, 12, 12, 5 Hz, 2H), 3.28 (dd, *J* = 8.3, 5.4 Hz, 1H), 3.35 (m, 1H), 3.61 (m, 3H), 3.86 (br dd, *J* = 7, 7 Hz, 1H), 3.92 (br dd, *J* = 7, 7 Hz, 1H), 4.09 (br dd, *J* = 11.6, 3.7 Hz, 2H), 4.90 (m, obscured

by water peak, 1H assumed), 4.98 (tt, *J* = 11.6, 4.3 Hz, 1H), 7.19 (m, 2H), 7.28 (m, 1H), 8.03 (s, 1H).

2-Fluoro-4-[(1-{1-[4-oxo-1-(tetrahydro-2H-pyran-4-yl)-4,5-dihydro-1H-pyrazolo[3,4-d]pyrimidin-6-yl]ethyl}azetidin-3-yl)oxy]-benzonitrile (10e). Prepared according to the same method as example **10g** except using 2-fluoro-4-hydroxybenzonitrile and heating for 1 h in the microwave at 140 °C and 75W. LCMS *m/z* 439.4 (M + 1). ¹H NMR (400 MHz, CD₃OD) δ 1.37 (d, *J* = 6.6 Hz, 3H), 1.89 (m, 2H), 2.29 (m, 2H), 3.31 (m, 1H, assumed, obscured by solvent peak), 3.38 (dd, *J* = 8.3, 5.0 Hz, 1H), 3.62 (m, 3H), 3.87 (dd, *J* = 7.1, 7.1 Hz, 1H), 3.94 (dd, *J* = 7.0, 7.0 Hz, 1H), 4.09 (br d, *J* = 11.6 Hz, 2H), 4.97 (m, 2H), 6.85 (m, 2H), 7.66 (dd, *J* = 8.1, 8.1 Hz, 1H), 8.03 (s, 1H).

2-Chloro-4-[(1-{1-[4-oxo-1-(tetrahydro-2H-pyran-4-yl)-4,5-dihydro-1H-pyrazolo[3,4-d]pyrimidin-6-yl]ethyl}azetidin-3-yl)oxy]-benzonitrile (10f). Same procedure as example **10g** except using 2-chloro-4-hydroxybenzonitrile. LCMS *m/z* 455.3 (M + 1). ¹H NMR (400 MHz, CD₃OD) δ 1.38 (d, *J* = 6.6 Hz, 3H), 1.89 (m, 2H), 2.29 (m, 2H), 3.31 (m, 1H, assumed, obscured by solvent peak), 3.38 (dd, *J* = 8.1, 5.2 Hz, 1H), 3.61 (m, 3H), 3.87 (dd, *J* = 7.1, 7.1 Hz, 1H), 3.93 (dd, *J* = 7.1, 7.1 Hz, 1H), 4.09 (m, 2H), 4.98 (m, 2H), 6.95 (dd, *J* = 8.7, 2.5 Hz, 1H), 7.11 (d, *J* = 2.5 Hz, 1H), 7.71 (d, *J* = 8.7 Hz, 1H), 8.03 (s, 1H).

Library Protocol for O-Substituted 6-[1-(3-Hydroxyazetidin-1-yl)ethyl]-1-(tetrahydro-2H-pyran-4-yl)-1,5-dihydro-4H-pyrazolo[3,4-d]pyrimidin-4-ones (10b and 10c). To the appropriate phenol (0.1 mmol) was added **14b** (20 mg, 0.05 mmol) in dimethylformamide (0.77 mL). Cesium carbonate (49 mg, 0.15 mmol) was added, and the reactions were heated to 70 °C for 20 h. The reactions were cooled to room temperature, and ethyl acetate (2 mL) was added, after which the reactions were heated to 35 °C and shaken. Reactions were centrifuged to segregate particulates, and 2.4 mL of the reaction mixtures was transferred to SCX-SPE columns. An additional 2.4 mL of ethyl acetate was added to the reaction vessel and transferred to the SCX-SPE column. The columns were washed with methanol (5 mL), and the desired products were then released by eluting with a solution of triethylamine in methanol (6 mL). The solvent was removed in vacuo. A solution of trifluoroacetic acid in dichloromethane (10%, 0.5 mL) was added, and the mixtures were shaken for 15 min. Solvents were removed in vacuo, and the crude samples were dissolved in dimethyl sulfoxide (0.6 mL) and purified by preparative HPLC (column: Xterra PrepMS C₁₈, 5 μm, 19 mm × 100 mm; solvent A, 0.1% trifluoroacetic acid in water (v/v); solvent B, acetonitrile; gradient 5−95% B), to afford the final examples **10b** and **10c**.

6-{1-[3-(2,5-Difluorophenoxy)azetidin-1-yl]ethyl}-1-(tetrahydro-2H-pyran-4-yl)-1,5-dihydro-4H-pyrazolo[3,4-d]pyrimidin-4-one, Trifluoroacetate Salt (10b). Library protocol provided 5.17 mg of **10d** with a retention time of 2.61 min. HPLC purity 89%. LCMS *m/z* 432.1 (M + 1).

6-{1-[3-(3-Chloro-4-fluorophenoxy)azetidin-1-yl]ethyl}-1-(tetrahydro-2H-pyran-4-yl)-1,5-dihydro-4H-pyrazolo[3,4-d]pyrimidin-4-one, Trifluoroacetate Salt (10c). Library protocol provided 1.9 mg of **10e** with a retention time of 2.77 min. HPLC purity 94%. LCMS *m/z* 448 (M + 1).

6-{1-[3-(Pyrimidin-2-yloxy)azetidin-1-yl]ethyl}-1-(tetrahydro-2H-pyran-4-yl)-1,5-dihydro-4H-pyrazolo[3,4-d]pyrimidin-4-one (15). Step 1: tert-Butyl 3-(Pyrimidin-2-yloxy)azetidine-1-carboxylate. A mixture of *N*-BOC-3-hydroxyazetidine (0.50 g, 2.9 mmol), 2-chloropyrimidine (0.33 g, 2.9 mmol), and potassium *tert*-butoxide (0.49 g, 4.3 mmol) in THF (20 mL) was heated to reflux for 6 h and then concentrated. The residue was diluted with water and extracted with methylene chloride. The organic extract was washed with brine, dried over MgSO₄, filtered, concentrated, and chromatographed (eluant 10:1 heptanes/ethyl acetate) to provide 508 mg of the titled compound. ¹H NMR (400 MHz, CDCl₃) δ 1.42 (s, 9H), 4.02 (m, 2H), 4.30 (m, 2H), 5.29 (m, 1H), 6.97 (t, *J* = 4.9 Hz, 1H), 8.50 (d, *J* = 4.9 Hz, 2H).

Step 2: 6-{1-[3-(Pyrimidin-2-yloxy)azetidin-1-yl]ethyl}-1-(tetrahydro-2H-pyran-4-yl)-1,5-dihydro-4H-pyrazolo[3,4-d]pyrimidin-4-one (15). To a solution of *tert*-butyl 3-(pyrimidin-2-yloxy)azetidine-1-carboxylate (150 mg, 0.6 mmol) in methylene chloride (2 mL) was added trifluoroacetic acid (0.154 mL). The mixture was stirred at room

temperature overnight and then concentrated. Acetonitrile (10 mL) was added to the resulting residue, followed by the addition of potassium carbonate (552 mg, 4 mmol) and 6-(1-bromoethyl)-1-(tetrahydro-2*H*-pyran-4-yl)-1,5-dihydro-4*H*-pyrazolo[3,4-*d*]pyrimidin-4-one (**6b**, 131 mg, 0.4 mmol). The reaction mixture was stirred at room temperature for 2 h and then heated to 90 °C for 3 h and concentrated. The residue was partitioned between water and methylene chloride. The organic layer was separated, washed with brine, dried over magnesium sulfate, filtered, concentrated, and chromatographed (eluant 200:1 chloroform/methanol) to provide 88 mg of **15** as a solid. LCMS *m/z* 398.0 (M + 1). ^{1}H NMR (400 MHz, CDCl$_3$) δ 1.34 (d, 3H, *J* = 7.0), 1.88−1.92 (m, 2H), 2.30−2.41 (m, 2H), 3.24 (br m, 1H), 3.40 (br m, 1H), 3.55 (br m, 3H), 3.60 (t, 2H, *J* = 11.6), 3.91 (br m, 2H), 4.12 (dd, 2H, *J* = 3.9, 11.4), 4.78−4.86 (m, 1H), 5.24−5.30 (m, 1H), 6.97 (t, 1H, *J* = 4.8), 8.05 (s, 1H), 8.49 (d, 2H, *J* = 5.0), 9.85 (br s, 1H). ^{13}C NMR (100 MHz, CDCl$_3$) δ 18.14, 32.17, 53.73, 58.49, 60.30, 65.20, 65.32, 67.00, 105.28, 115.63, 134.74, 151.76, 157.75, 159.41.

1-(Cyclopentyl)-6-{(1R)-1-[3-(pyrimidin-2-yloxy)azetidin-1-yl]-ethyl}-1,5-dihydro-4H-pyrazolo[3,4-d]pyrimidin-4-one (**16**). A mixture of **13a** (500 mg, 1.65 mmol), 2-chloropyrimidine (189 mg, 1.65 mmol), and potassium *t*-butoxide (388 mg, 3.46 mmol) in THF (10 mL) was heated to reflux for 8 h. The mixture was cooled and concentrated. The resulting residue was diluted with water and extracted with methylene chloride. The combined extracts were washed with brine, dried over MgSO$_4$, filtered, concentrated, and chromatographed (gradient elution of 200:1 to 100:1 CHCl$_3$−CH$_3$OH) to give 130 mg of a solid. The 130 mg of enantio-enriched solid was separated by SFC chromatography using a Chiralcel AS-H column (4.6 mm × 25 cm) with a mobile phase of 90/10 carbon dioxide/methanol and a flow of 2.5 mL/min. The desired first enantiomer peak had a retention time of 6.65 min. The solid was further repurified by standard chromatography (eluant 100:1 chloroform/methanol) to yield 68 mg (100% ee) of **16** as a solid. LCMS *m/z* 382.2 (M + 1). ^{1}H NMR (400 MHz, CDCl$_3$) δ 1.36 (d, 3H, *J* = 5.0), 1.63−1.76 (m, 2H), 1.88−2.16 (m, 6H), 3.29 (br s, 1H), 3.45 (br s, 1H), 3.58 (br s, 1H), 3.94 (br s, 2H), 5.15 (apparent quintet, 1H, *J* = 7.5), 5.25−5.31 (m, 1H), 6.97 (t, 1H, *J* = 4.8), 8.03 (s, 1H), 8.49 (d, 2H, *J* = 4.6), 9.85 (br s, 1H).

2-((1-Benzhydrylazetidin-3-yl)oxy)pyrimidine (**17**). To a suspension of sodium hydride (762 mg of a 60% dispersion in oil, 19 mmol) and THF (9 mL) was added 1-(diphenylmethyl)-3-hydroxyazetidine (1.50 g, 6.27 mmol). After 10 min, gas evolution ceased and 2-chloropyrimidine was added. The reaction mixture was heated to 50 °C overnight and then cooled. The mixture was partitioned between water (50 mL) and EtOAc (100 mL). The separated organic layer was washed with water (50 mL) and brine (50 mL), concentrated, and chromatographed (eluant 80:20 heptanes/ethyl acetate) to provide 1.99 g of **17** as a solid. LCMS *m/z* 318.0 (M + 1). ^{1}H NMR (400 MHz, CDCl$_3$) δ 3.19 (br s, 2H), 3.80 (br s, 2H), 4.48 (br s, 1H), 5.24−5.32 (m, 1H), 6.88−6.91 (m, 1H), 7.16−7.20 (m, 2H), 7.25−7.29 (m, 4H), 7.42−7.44 (m, 4H), 8.44 (d, *J* = 4.6 Hz, 2H).

1-(3-(Benzhydrylamino)-2-hydroxypropyl)pyrimidin-2(1H)-one (**18**). A mixture of **17** (100 mg, 0.315 mmol), 1N HCl (0.317 mL, 0.317 mmol), and water (1.68 mL) was stirred overnight at room temperature. The mixture was divided in half and to one-half was added additional aqueous HCl (0.16 mL of 1N, 0.16 mmol) and the mixture was stirred for 3 days, at which point LCMS showed an approximate ratio of **17**/**18** of 1:2. The mixture was stirred for another 4 days, concentrated and partitioned between 1N NaOH (1 mL) and ethyl acetate (2 mL). The organic layer was concentrated and purified by LCMS to provide **18**. LCMS *m/z* 336.1 (M + 1). ^{1}H NMR (400 MHz, CD$_3$OD) δ 3.00 (dd, 1H, *J* = 10.0, 12.9), 3.14 (dd, 1H, *J* = 3.3, 12.9), 3.76 (dd, 1H, *J* = 7.9, 13.3), 4.18 (dd, 1H, *J* = 3.1, 13.5), 4.35−4.43 (m, 1H), 5.60 (s, 1H), 6.58−6.61 (m, 1H), 7.38−7.55 (m, 10H), 8.15−8.17 (m, 1H), 8.63 (br s, 1H). IR: 1670, 1200, 1132 cm^{-1}.

1-Cyclopentyl-6-[(1R)-1-(3-pyrimidin-2-ylazetidin-1-yl)ethyl]-1,5-dihydro-4H-pyrazolo[3,4-d]pyrimidin-4-one (**19**). *a.* *2-(Azetidin-3-yl)pyrimidine Bis-methanesulfonate*. Step 1. A solution of *tert*-butyl 3-hydroxyazetidine-1-carboxylate (97%, 5.0 g, 28 mmol) in dichloro-

methane (50 mL) was treated with triethylamine (7.8 mL, 56 mmol) and cooled to 0 °C. A solution of methanesulfonyl chloride (2.28 mL, 29.3 mmol) in dichloromethane was added dropwise to the cold reaction, which was maintained at 0 °C for 2 h and then allowed to warm to room temperature over the next 18 h. Solvents were removed in vacuo, and the residue was taken up in ether and filtered. The filtrate was concentrated in vacuo, and the residue purified via silica gel chromatography (eluant: 5:1 heptane/ethyl acetate, then 2:1 heptane/ethyl acetate) to provide *tert*-butyl 3-[(methylsulfonyl)oxy]azetidine-1-carboxylate as a solid. Yield: 6.5 g, 26.0 mmol, 93%. LCMS *m/z* 503.1 (2M + 1). ^{1}H NMR (400 MHz, CDCl$_3$) δ 1.44 (s, 9H), 3.06 (s, 3H), 4.09 (ddd, *J* = 10.4, 4.2, 1.2, 2H), 4.27 (ddd, *J* = 10.4, 6.6, 1.2 Hz, 2H), 5.19 (tt, *J* = 6.6, 4.2 Hz, 1H). ^{13}C NMR (100 MHz, CDCl$_3$) δ 28.23, 38.33, 56.45 (br), 67.25, 80.29, 155.80.

Step 2. Potassium iodide (12.9 g, 77.7 mmol) and *tert*-butyl 3-[(methylsulfonyl)oxy]azetidine-1-carboxylate (6.5 g, 26.0 mmol) were combined in dimethylformamide (40 mL). The reaction mixture was stirred at 110 °C for 16 h and then concentrated in vacuo, diluted with water, and extracted with ethyl acetate. The combined organic layers were washed with water and then washed with saturated aqueous sodium chloride solution and dried over magnesium sulfate. Filtration and removal of solvent in vacuo gave a residue, which was purified by silica gel chromatography (eluant: 4:1 heptane/ethyl acetate) to afford *tert*-butyl 3-iodoazetidine-1-carboxylate as a solid. Yield: 6.2 g, 21.9 mmol, 84%. LCMS *m/z* 284.0 (M + 1). ^{1}H NMR (400 MHz, CDCl$_3$) δ 1.43 (s, 9H), 4.28 (m, 2H), 4.46 (m, 1H), 4.64 (m, 2H). ^{13}C NMR (100 MHz, CDCl$_3$) δ 2.57, 28.27, 61.49, 80.09, 155.52.

Step 3. Zinc powder (150.1 g, 2.30 mol) and molecular sieves (50 g) were combined in a reaction flask and flame-dried under vacuum for 10 min. Once the flask had returned to room temperature, it was charged with tetrahydrofuran (4 L), and 1,2-dibromoethane (24.4 mL, 0.28 mol) was added. The reaction mixture was heated to 50 °C for 10 min and then allowed to come to ambient temperature, at which time trimethylsilyl chloride (33.5 mL, 0.264 mol) was added (*Caution: slightly exothermic*). The mixture was allowed to stir at room temperature for about 18 h. Slow addition of *tert*-butyl 3-iodoazetidine-1-carboxylate (500 g, 1.77 mol) over 1.5 h was followed by stirring for an additional 18 h. In a separate flask, 2-bromopyrimidine (253 g, 1.59 mol) was combined with molecular sieves (85 g) in tetrahydrofuran (1.3 L), and the mixture was degassed. This mixture was treated with tetrakis(triphenylphosphine)-palladium(0) (32.7 g, 0.0283 mol) and then added to the flask containing the reaction mixture from *tert*-butyl 3-iodoazetidine-1-carboxylate. The reaction was stirred for 25 h and then filtered through Celite. The filtrate was concentrated under reduced pressure and then partitioned between saturated aqueous sodium carbonate solution (2 L) and ethyl acetate (2 L). The aqueous layer was extracted with ethyl acetate (2 × 2 L), and the combined organic layers were dried over sodium sulfate and concentrated in vacuo. The resulting yellow liquid residue was triturated with methyl *tert*-butyl ether (500 mL), and the precipitate was removed by filtration. Partial concentration of the filtrate resulted in precipitation of a solid; the mixture at this point was cooled in an ice−water bath. Filtration then provided a solid, which was washed with a minimum quantity of cold methyl *tert*-butyl ether to afford *tert*-butyl 3-pyrimidin-2-ylazetidine-1-carboxylate as a white solid, which was taken directly into the next step. Yield: 131 g, 0.557 mol, 31%. GCMS *m/z* 180 ([M − *tert*-butyl] + 1); 136 ([M − BOC] + 1). ^{1}H NMR (300 MHz, CDCl$_3$) δ 1.45 (s, 9H), 4.0 (m, 1H), 4.3 (m, 4H), 7.2 (t, 1H), 8.75 (d, 2H).

Step 4. Methanesulfonic acid (108.3 mL, 1.67 mol) was added to an ice-cold solution of *tert*-butyl 3-pyrimidin-2-ylazetidine-1-carboxylate (131 g, 0.557 mol, from previous step) in dichloromethane/dioxane (9:1 ratio, 1 L). The mixture was allowed to warm to room temperature over about 18 h with stirring. The precipitate was filtered and washed with methyl *tert*-butyl ether to provide 2-(azetidin-3-yl)pyrimidine dimethylsulfonate as a white solid. Yield: 180 g, 0.550 mol, 99%. LCMS *m/z* 136.2 (M + 1). ^{1}H NMR (300 MHz, D$_2$O) δ 2.55 (s, 6H), 4.33 (m, 5H), 7.64 (t, *J* = 5.3 Hz, 1H), 8.90 (d, *J* = 5.2 Hz, 2H). ^{13}C NMR (75 MHz, D$_2$O) δ 36.47, 38.53, 49.98, 121.63, 158.08, 164.37.

b. 1-Cyclopentyl-6-[(1R)-1-(3-pyrimidin-2-ylazetidin-1-yl)ethyl]-1,5-dihydro-4H-pyrazolo[3,4-d]pyrimidin-4-one (19). Compound **12a** (35 g, 107 mmol) and 2-(azetidin-3-yl)pyrimidine dimethylsulfonate (38.62 g, 118 mmol) were mixed with acetonitrile (700 mL), and the heterogeneous reaction mixture was treated with triethylamine (134 mL, 961 mmol) and heated to 80 °C for 3.5 h. The reaction became homogeneous and light yellow. The product was concentrated by distillation at a pot temperature of 80–90 °C, until 350–500 mL of acetonitrile remained. It was then allowed to crystallize as it cooled to room temperature. The mixture was stirred for about 18 h and then filtered to obtain **19** as a solid. Yield: 21 g, 57.5 mmol, 54%. For samples of **19** prepared under similar conditions, but chromatographed rather than crystallized, the minor enantiomer of the product was removed by chiral chromatography using a Chiralpak AD-H column (5 μm; 2.1 cm × 25 cm; mobile phase, 70:30 carbon dioxide/methanol; flow rate 65 g/min). Compound **19** was the second-eluting enantiomer, retention time approximately 3.35 min. LCMS m/z 366.2 (M + 1). ^{1}H NMR (400 MHz, CDCl$_3$) δ 1.33 (d, J = 6.6 Hz, 3H), 1.72 (m, 2H), 1.97 (m, 2H), 2.11 (m, 4H), 3.58 (m, 2H), 3.71 (dd, J = 7.1, 7.1 Hz, 1H), 3.79 (m, 2H), 4.00 (m, 1H), 5.16 (m, 1H), 7.19 (t, J = 4.9 Hz, 1H), 8.05 (s, 1H), 8.72 (d, J = 5.0 Hz, 2H), 9.86 (br s, 1H). ^{13}C NMR (100 MHz, CDCl$_3$) δ 18.07, 24.73, 32.38, 32.45, 37.61, 56.69, 57.69, 57.78, 65.09, 105.09, 119.00, 134.54, 157.11, 157.93, 160.39, 169.82 (one aromatic signal not observed).

ASSOCIATED CONTENT

Ⓢ Supporting Information

Data table for PDE9 IC$_{50}$ values on key compound. LC/MS data for presence of α-chloro intermediate in amine displacement of **12b** when using the amine-HCl salt. This material is available free of charge via the Internet at http://pubs.acs.org.

Accession Codes

All coordinates have been deposited and will be released upon publication.

AUTHOR INFORMATION

Corresponding Author

*: michelle.m.claffey@pfizer.com, 860-715-3416; chris.j.helal@pfizer.com, 860-715-5064.

Notes

The authors declare no competing financial interest.

ABBREVIATIONS USED

PDE:phosphodiesterase; C_{bu}:unbound brain concentration; cGMP:cyclic guanosine monophosphate; cAMP:cyclic adenosine monophosphate; CSF:cerebrospinal fluid; fu$_p$:fraction unbound in plasma; fu$_{mic}$:fraction unbound in microsomes; K_m:Michallis constant; LE:ligand efficiency; MDR BA/AB:ratio of basal to apical (BA) to apical to basal (AB) transport in MDR1A overexpressing canine kidney cells; MPO:multiparametric optimization; MW:molecular weight; TPSA:topological polar surface area; HLM Cl:human liver microsomal clearance (mL/min/kg); P-gp:P-glycoprotein; Cpu:unbound plasma concentration

REFERENCES

(1) (a) Verhoest, P. R.; Chapin, D. S.; Corman, M.; Fonseca, K.; Harms, J. F.; Hou, X.; Marr, E. S.; Menniti, F. S.; Nelson, F.; O'Connor, R.; Pandit, J.; Proulx-LaFrance, C.; Schmidt, A. W.; Schmidt, C. J.; Suiciak, J. A.; Liras, S. Discovery of a Novel Class of Phosphodiesterase 10A Inhibitors and Identification of Clinical Candidate 2-[4-(1-Methyl-4-pyridin-4-yl-1H-pyrazol-3-yl)-phenoxymethyl]-quinoline (PF-2545920)(I) for the Treatment of Schizophrenia. *J. Med. Chem.* **2009**, *52*, 5188–5196. (b) Chappie, T. A.; Humphrey, J. M.; Allen, M. P.; Estep, K. G.; Fox, C. B.; Lebel, L. A.;

Liras, S.; Marr, E. S.; Menniti, F. S.; Pandit, J.; Schmidt, C. J.; Tu, M.; Williams, R. D.; Yang, F. V. Discovery of a Series of 6,7-Dimethoxy-4-pyrrolidylquinazoline PDE10A Inhibitors. *J. Med. Chem.* **2007**, *50*, 182–185.

(2) (a) Andreeva, S. G.; Dikkes, P.; Epstein, P. M.; Rosenberg, P. A. Expression of cGMP-specific phosphodiesterase 9A mRNA in the rat brain. *J. Neurosci.* **2001**, *21*, 9068–9076. (b) Fisher, D. A.; Smith, J. F.; Pillar, J. S.; St. Denis, S. H.; Cheng, J. B. Isolation and characterization of PDE9A, a novel human cGMP-specific phosphodiesterase. *J. Biol. Chem.* **1998**, *273*, 15559–15564.

(3) (a) Kleiman, R. J.; Chapin, D. S.; Christoffersen, C.; Freeman, J.; Fonseca, K. R.; Geoghegan, K. F.; Grimwood, S.; Guanowsky, V.; Hajos, M.; Harms, J. F.; Helal, C. J.; Hoffmann, W. E.; Kocan, G. P.; Majchrzak, M. J.; McGinnis, D.; McLean, S.; Menniti, F. S.; Nelson, F.; Roof, R.; Schmidt, A. W.; Seymour, P. A.; Stephenson, D. T.; Tingley, F. D.; Vanase-Frawley, M.; Verhoest, P. R.; Schmidt, C. J. Phosphodiesterase 9A regulates central cGMP and modulates responses to cholinergic and monoaminergic perturbation in vivo. *J. Pharmacol. Exp. Ther.* **2012**, *341*, 396–409. (b) Hutson, P. H.; Finger, E. N.; Magliaro, B. C.; Smith, S. M.; Converso, A.; Sanderson, P. E.; Mullins, D.; Hyde, L. A.; Eschle, B. K.; Turnbull, Z.; Sloan, H.; Guzzi, M.; Zhang, X.; Wang, A.; Rindgen, D.; Mazzola, R.; Vivian, J. A.; Eddins, D.; Uslaner, J. M.; Bednar, R.; Gambone, C.; Le-Mair, W.; Marino, M. J.; Sachs, N.; Xu, G.; Parmentier-Batteur, S. The selective phosphodiesterase 9 (PDE9) inhibitor PF-04447943 (6-[(3S,4S)-4-methyl-1-(pyrimidin-2-ylmethyl)pyrrolidin-3-yl]-1-(tetrahydro-2H-pyran-4-yl)-1,5-dihydro-4H-pyrazolo[3,4-d]pyrimidin-4-one) enhances synaptic plasticity and cognitive function in rodents. *Neuropharmacology* **2011**, *61*, 665–676. (c) Vardigan, J. D.; Converso, A.; Hutson, P. H.; Uslaner, J. M. The Selective Phosphodiesterase 9 (PDE9) Inhibitor PF-04447943 Attenuates a Scopolamine-Induced Deficit in a Novel Rodent Attention Task. *J. Neurogenet.* **2011**, *25*, 120–126. (d) Halene, T. B.; Siegel, S. J. PDE inhibitors in psychiatry—future options for dementia, depression and schizophrenia? *Drug Discovery Today* **2007**, *12*, 870–878. (e) Reneerkens, O. A. H.; Rutten, K.; Steinbusch, H. W. M.; Blokland, A.; Prickaerts, J. Selective phosphodiesterase inhibitors: a promising target for cognition enhancement. *Psychopharmacology (Berlin, Ger.)* **2009**, *202*, 419–443. (f) Schmidt, C. J. Phosphodiesterase inhibitors as potential cognition enhancing agents. *Curr. Top. Med. Chem.* **2010**, *10*, 222–230. (g) Siuciak, J. A. The role of phosphodiesterases in schizophrenia: therapeutic implications. *CNS Drugs* **2008**, *22*, 983–993. (h) van der Staay, F. J.; Rutten, K.; Baerfacker, L.; DeVry, J.; Erb, C.; Heckroth, H.; Karthaus, D.; Tersteegen, A.; van Kampen, M.; Blokland, A.; Prickaerts, J.; Reymann, K. G.; Schroeder, U. H.; Hendrix, M. The novel selective PDE9 inhibitor BAY 73–6691 improves learning and memory in rodents. *Neuropharmacology* **2008**, *55*, 908–918.

(4) Verhoest, P. R.; Proulx-Lafrance, C.; Corman, M.; Chenard, L.; Helal, C. J.; Hou, X.; Kleiman, R.; Liu, S.; Marr, E.; Menniti, F. S.; Schmidt, C. J.; Vanase-Frawley, M.; Schmidt, A. W.; Williams, R. D.; Nelson, F. R.; Fonseca, K. R.; Liras, S. Identification of a brain penetrant PDE9A inhibitor utilizing prospective design and chemical enablement as a rapid lead optimization strategy. *J. Med. Chem.* **2009**, *52*, 7946–7949.

(5) Hopkins Andrew, L.; Groom Colin, R.; Alex, A. Ligand efficiency: a useful metric for lead selection. *Drug Discovery Today* **2004**, *9*, 430–431.

(6) (a) Gleeson, M. P. Generation of a Set of Simple, Interpretable ADMET Rules of Thumb. *J. Med. Chem.* **2008**, *51*, 817–834. (b) Hitchcock, S. A. Structural Modifications that Alter the P-Glycoprotein Efflux Properties of Compounds. *J. Med. Chem.* **2012**, *55*, 4877–4895.

(7) Wager, T. T.; Chandrasekaran, R. Y.; Hou, X.; Troutman, M. D.; Verhoest, P. R.; Villalobos, A.; Will, Y. Defining Desirable Central Nervous System Drug Space through the Alignment of Molecular Properties, in Vitro ADME, and Safety Attributes. *ACS Chem. Neurosci.* **2010**, *1*, 420–434.

(8) Hughes, J. D.; Blagg, J.; Price, D. A.; Bailey, S.; DeCrescenzo, G. A.; Devraj, R. V.; Ellsworth, E.; Fobian, Y. M.; Gibbs, M. E.; Gilles, R.

W.; Greene, N.; Huang, E.; Krieger-Burke, T.; Loesel, J.; Wager, T.; Whiteley, L.; Zhang, Y. Physiochemical drug properties associated with in vivo toxicological outcomes. *Bioorg. Med. Chem. Lett.* **2008**, *18*, 4872−4875.

(9) Verhoest, P. R.; Fonseca, K. R.; Hou, X.; Proulx-LaFrance, C.; Corman, M.; Helal, C. J.; Claffey, M. M.; Tuttle, J.; Coffman, K. J.; Liu, S.; Nelson, F.; Kleiman, R. J.; Menniti, F. S.; Schmidt, C. J.; Vanase-Frawley, M.; Liras, S. Design and Discovery of 6-[(3*S*,4*S*)-4-Methyl-1-(pyrimidin-2-ylmethyl)pyrrolidin-3-yl]-1-(tetrahydro-2*H*-pyran-4-yl)-1,5-dihydro-4*H*-pyrazolo[3,4-*d*]pyrimidin-4-one (PF-04447943), a Selective Brain Penetrant PDE9A Inhibitor for the Treatment of Cognitive Disorders, *J. Med. Chem.*, **2012**, DOI http://pubs.acs.org/doi/abs/10.1021/jm3007799.

(10) Murphy, S. T.; Case, H. L.; Ellsworth, E.; Hagen, S.; Huband, M.; Joannides, T.; Limberakis, C.; Marotti, K. R.; Ottolini, A. M.; Rauckhorst, M.; Starr, J.; Stier, M.; Taylor, C.; Zhu, T.; Blaser, A.; Denny, W. A.; Lu, G.-L.; Smaill, J. B.; Rivault, F. The synthesis and biological evaluation of novel series of nitrile-containing fluoroquinolones as antibacterial agents. *Bioorg. Med. Chem. Lett.* **2007**, *17*, 2150−2155.

(11) Hoffmann, R. W. Allylic 1,3-strain as a controlling factor in stereoselective transformations. *Chem. Rev.* **1989**, *89*, 1841−1860.

(12) (a) Sadowski, J.; Gasteiger, J.; Klebe, G. Comparison of Automatic Three-Dimensional Model Builders Using 639 X-Ray Structures. *J. Chem. Inf. Comput. Sci.* **1994**, *34*, 1000−1008. (b) The 3-D structure generator CORINA is available from Molecular Networks GmbH, Erlangen, Germany (http://www.molecular-networks.com).

(13) Gehlhaar, D. K.; Verkhivker, G. M.; Rejto, P. A.; Sherman, C. J.; Fogel, D. B.; Fogel, L. J.; Freer, S. T. Molecular Recognition of the Inhibitor AG-1343 by HIV-1 Protease: Conformationally Flexible Docking by Evolutionary Programming. *Chem. Biol.* **1995**, *2*, 317−324.

(14) Marrone, T. J.; Luty, B. A.; Rose, P. W. Discovering High-Affinity Ligands from the Computationally Predicted Structures and Affinities of Small Molecules Bound to A Target: A Virtual Screening Approach. *Perspect. Drug Discovery Des.* **2000**, *20*, 209−230.

(15) Feng, B.; Mills, J. B.; Davidson, R. E.; Mireles, R. J.; Janiszewski, J. S.; Troutman, M. D.; de Morais, S. M. In vitro P-glycoprotein assays to predict the in vivo interactions of P-glycoprotein with drugs in the central nervous system. *Drug Metab. Dispos.* **2008**, *36*, 268−275.

(16) Wager, T. T.; Hou, X.; Verhoest, P. R.; Villalobos, A. Moving beyond Rules: The Development of a Central Nervous System Multiparameter Optimization (CNS MPO) Approach To Enable Alignment of Druglike Properties. *ACS Chem. Neurosci.* **2010**, *1*, 435−449.

(17) For a recent review on methods used to pre-clinically evaluate brain penetration of compounds, see: Shaffer, C. L. Defining neuropharmacokinetic parameters in CNS drug discovery to determine cross-species pharmacologic exposure−response relationships. *Annu. Rep. Med. Chem.* **2010**, *45*, 55−70.

(18) Choi, S.-W.; Elmaleh, D. R.; Hanson, R. N.; Shoup, T. M.; Fischman, A. J. Novel (bisarylmethoxy)butylpiperidine analogues as neurotransmitter transporter inhibitors with activity at dopamine receptor sites. *Bioorg. Med. Chem.* **2002**, *10*, 4091−4102.

(19) Chang, G.; Steyn, S. J.; Umland, J. P.; Scott, D. O. Strategic Use of Plasma and Microsome Binding To Exploit in Vitro Clearance in Early Drug Discovery. *ACS Med. Chem. Lett.* **2010**, *1*, 50−53.

(20) Nicholas, T; Evans, R; Styren, S; Qui, R; Wang, E. Q.; Nelson, F; Le, V; Grimwood, S; Christoffersen, C; Banerjee, S; Corrigan, B.; Kocan, G.; Geoghegan, K.; Carrieri, C.; Raha, N.; Verhoest, P.; Soares, H. (2009) PF-04447943, a novel PDE9A inhibitor, increases cGMP levels in cerebrospinal fluid: translation from non-clinical species to healthy human volunteers. *Alzheimer's Dementia* **2009**, *5*, P330.

(21) Ranatunge, R. R.; Augustyniak, M.; Bandarage, U. K.; Earl, R. A.; Ellis, J. L.; Garvey, D. S.; Janero, D. R.; Letts, L. G.; Martino, A. M.; Murty, M. G.; Richardson, S. K.; Schroeder, J. D.; Shumway, M. J.; Tam, S. W.; Trocha, A. M.; Young, D. V. Synthesis and Selective Cyclooxygenase-2 Inhibitory Activity of a Series of Novel, Nitric Oxide Donor-Containing Pyrazoles. *J. Med. Chem.* **2004**, *47*, 2180−2193.